

# Interference Mitigation via Relaying

S. Arvin Ayoughi, Wei Yu, *Fellow, IEEE*

**Abstract**—This paper studies the effectiveness of relaying for interference mitigation in an interference-limited communication scenario. We are motivated by the observation that in a cellular network, a relay node placed at the cell edge observes a combination of intended signal and inter-cell interference that is correlated with the received signal at a nearby destination, so a relaying link can effectively allow the antennas at the relay and at the destination to be pooled together for both signal enhancement and interference mitigation. We model this scenario by a multiple-input multiple-output (MIMO) Gaussian relay channel with a digital relay-to-destination link of finite capacity, and with *correlated* noise across the relay and destination antennas. Assuming a compress-and-forward strategy with Gaussian input distribution and quantization noise, we propose a coordinate ascent algorithm for obtaining a stationary point of the non-convex joint optimization of the transmit and quantization covariance matrices. For fixed input distribution, the globally optimum quantization noise covariance matrix can be found in closed-form using a transformation of the relay's observation that simultaneously diagonalizes two conditional covariance matrices by congruence. For fixed quantization, the globally optimum transmit covariance matrix can be found via convex optimization. This paper further shows that such an optimized achievable rate is within a constant additive gap of the MIMO relay channel capacity. The optimal structure of the quantization noise covariance enables a characterization of the slope of the achievable rate as a function of the relay-to-destination link capacity. Moreover, this paper shows that the improvement in spatial degrees of freedom by MIMO relaying in the presence of noise correlation is related to the aforementioned slope via a connection to the deterministic relay channel.

**Index Terms**—Gaussian MIMO relay channel, noise correlation, compress-and-forward, deterministic relay channel, reverse water-filling, dimension reduction, distributed interference zero-forcing, approximate capacity.

## I. INTRODUCTION

**I**NTERFERENCE is a main limiting factor for increasing data rates in many communication scenarios. A wireless cellular network with densely deployed basestations (BSs), for example, is typically interference limited. Provisioning of high data rates at cell edges, where signal is relatively weaker and interference is stronger, is a major challenge in cellular network physical layer design.

This paper explores the use of relays for interference mitigation. The idea is that by placing a multiple-antenna relay at the cell edge (see Fig. 1), a user device in close proximity of a relay would be able to establish an out-of-band

relaying link and benefit from relay's observation in decoding the downlink signal. Due to the physical proximity of the relay and the intended receiver, their observed interference signals are highly correlated. In essence, the relay and the intended receiver would be able to pool their antennas together using the relaying link. The extra spatial dimensions enables not only signal enhancement but also interference mitigation at the receiver.

The benefit of antenna pooling depends crucially on the quality of the relaying link. The goal of this paper is to quantify the benefit of relaying for downlink transmission of a cellular network as a function of the relaying link capacity. Toward this end, this paper studies a multiple-input multiple-output (MIMO) Gaussian relay channel with digital relaying link, where, due to common inter-cell interference, the noise processes across the relay and destination antennas are correlated. This is a simple yet fundamental model of cooperative communications for which information theoretical analysis can yield significant insight into the effectiveness of cooperative interference mitigation. In particular, this paper adopts a compress-and-forward relaying strategy, which is appropriate given the physical proximity of the relay and destination in the scenario of interest [1], [2]. In this case, the relay provides the destination with a compressed version of its observations, the accuracy of which is determined by the available capacity of the relaying link. The relay uses Wyner-Ziv coding to exploit the side information available at the destination in quantizing its observations. The goal of this paper is to analyze the optimal transmission and quantization strategies for the MIMO relay channel with digital relaying link in the presence of correlated interference.

### A. Main Results

This paper makes the following contributions toward the goal of understanding how to best take advantage of the MIMO relay for both signal enhancement and interference mitigation:

- We propose an iterative algorithm for optimizing the covariance matrices of Gaussian input signal and Gaussian quantization noise for the MIMO relay channel with correlated noise. We show that the optimization of input covariance matrix for fixed quantization noise distribution is a concave optimization, and the optimization of quantization noise covariance matrix for fixed input distribution can be solved via a simultaneous diagonalization transformation. Further, the allocation of relaying bits across the spatial dimensions should follow a reverse water-filling solution, where more bits are used to quantize spatial dimensions with higher conditional signal-to-interference-and-noise ratios (CSINRs).
- We characterize the slope of compress-and-forward achievable rate versus the relaying link capacity curve

This work was supported in part by Huawei Technologies Canada Co., Ltd., and in part by the Natural Sciences and Engineering Research Council (NSERC) of Canada. The materials in this paper have been presented in part at the IEEE International Conference on Communication (ICC), London, UK, June 2015, and in part at the 14<sup>th</sup> Canadian Workshop on Information Theory (CWIT), St. John's, NL, Canada, July 2015.

The authors are with The Edward S. Rogers Sr. Department of Electrical and Computer Engineering, University of Toronto, Toronto, Ontario M5S 3G4, Canada (e-mails: sa.ayoughi@mail.utoronto.ca, weiyu@comm.utoronto.ca).

for the optimized quantization noise covariance at a fixed input distribution. The slope is related to the generalized eigenvalues of certain conditional covariance matrices. One of the main results of this paper is that this slope can asymptotically approach the maximum value of 1, if the MIMO relay channel contains an asymptotically deterministic component.

- We characterize the improvement in the spatial degrees of freedom (DoF) by compress-and-forward relaying as a function of the number of antennas in the network. A distributed interference zero-forcing scheme at the relay is shown to be DoF optimal. The improvement in spatial DoF (assuming infinite relay link capacity) is shown to be equal to the number of asymptotically deterministic components in the channel. Thus, the existence of asymptotically deterministic components is the fundamental reason for the effectiveness of relaying for interference mitigation and signal enhancement.
- The optimized compress-and-forward strategy is shown to achieve the capacity of the MIMO relay channel with noise correlation to within a constant additive gap, which only depends on the number of antennas.

### B. Related Works

The relay channel is a classical model that has been widely studied in the literature. Specifically related to this work, relaying in the presence of noise correlation for single-input single-output (SISO) Gaussian channel is studied in [3], where the negative correlation between relay and destination noises is shown to improve the achievable rate of the compress-and-forward relaying scheme. For the Gaussian MIMO relay channel with independent noises, a coordinate ascent procedure for maximizing the compress-and-forward achievable rate over input and quantization noise covariance matrices is proposed in [4]. For optimizing quantization at the relay under fixed input distribution, [4] uses the Conditional Karhunen-Loève Transform (CKLT) [5] of the relay's observed vector given the destination's observation, followed by a reverse water-filling solution for quantization rate allocation. This paper focuses on the relay channel with correlated noises for which the solution is more complex. We show that the right transformation is the simultaneous diagonalization by \*congruence<sup>1</sup> [6] of two conditional covariance matrices of relay observation [7]. The optimal allocation of quantization rates again has a reverse water-filling interpretation, and is related to the generalized eigenvalues of the conditional covariance matrices. When noises are independent simultaneous diagonalization transform simplifies to the CKLT.

The optimization of quantization noise covariance is also solved in [8], but from a source coding perspective. In [8], canonical correlation analysis (CCA) is used to transform the relay observation before quantization. CCA can be interpreted as indirect simultaneous diagonalization by \*congruence of

<sup>1</sup>Here, "\*" refers to conjugate transpose of the transformation matrix. Although in this paper we use  $(\cdot)^{\dagger}$  to denote conjugate transpose, we preferred not to change the terminology of [6].

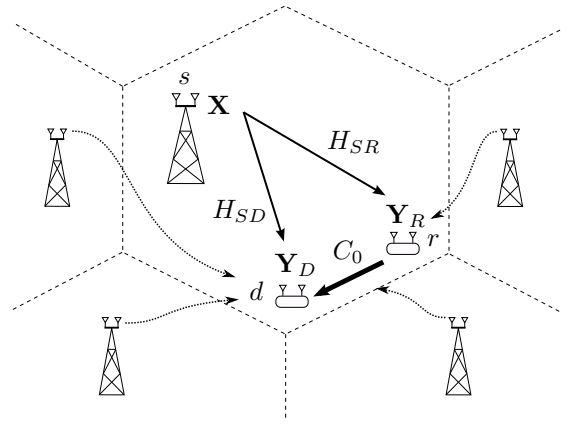


Fig. 1. A cellular network with a BS and a cell-edge user that is located close to a relay node. The relay pools antennas with the receiver through a finite-capacity digital link. Due to the common interference, the noise processes at the relay and at the destination antennas are correlated.

two conditional covariance matrices of the relay observation. Although our solution to the optimization problem can eventually be shown to be the same as that of [8], the direct diagonalization approach in this paper is simpler and provides insight into the optimized MIMO relaying strategy for interference mitigation and signal enhancement.

For the SISO Gaussian relay channel with noise correlation, [9] shows that compress-and-forward achieves the capacity to within a constant additive gap. For the MIMO Gaussian relay channel with independent noise vectors, capacity approximation using the partial decode-and-forward scheme is provided in [10] using partial decode-and-forward scheme. In this paper, for the MIMO Gaussian relay channel with noise correlation, we use the simultaneous diagonalization transform to show that compress-and-forward achieves the capacity to within a constant additive gap that is tighter than the gap of extension of [9] to the MIMO case.

This paper studies the improvement in spatial DoF due to the compress-and-forward relaying. The DoF-optimal transformation at the relay prior to quantization involves distributed zero-forcing of interference. Distributed zero-forcing of interference has been considered for various classes of SISO relay networks with analog relaying links, e.g., [11]–[14]. This paper deals with a MIMO relay channel with digital relaying link in which distributed zero-forcing of interference reveals the asymptotically deterministic components of the MIMO relay channel. The determinism here refers to the condition that the observation of the relay is a deterministic function of the input of the channel and the observation of the destination. As shown in [15], compress-and-forward achieves the cut-set upper bound in this case. This paper illustrates that this type of determinism occurs in the MIMO relay channel in the asymptotically high SNR and INR regime. This is the fundamental reason that compress-and-forward relaying can be effective in improving the overall throughput in a MIMO relay channel [16].

### C. Notation

In this paper, we denote matrices by uppercase letters, e.g.,  $H$ , vectors of random variables by uppercase bold letters, e.g.,  $\mathbf{X}$ , and its realization by lowercase bold letters, e.g.,  $\mathbf{x}$ . Also,  $\mathbf{0}_{r \times 1}$  stands for the  $r$ -dimensional zero vector and  $\mathbf{I}_r$  is the  $r \times r$  identity matrix. Conjugate transpose, Moore-Penrose pseudoinverse, trace, determinant, rank, the  $i^{\text{th}}$  largest eigenvalue, and the row span of a matrix are denoted by  $(\cdot)^\dagger$ ,  $(\cdot)^{-1}$ ,  $\text{tr}(\cdot)$ ,  $|\cdot|$ ,  $\text{rank}(\cdot)$ ,  $\lambda_i(\cdot)$ , and  $\text{rowspan}(\cdot)$ , respectively. For two matrices  $A$  and  $B$ ,  $A \succeq B$  means that  $A - B$  is positive semidefinite. The expectation operator is shown by  $\mathbb{E}(\cdot)$ . The set of complex numbers is denoted by  $\mathbb{C}$ . Finally, we define  $(x)^+ = \max(0, x)$ .

### D. Organization of the Paper

Section II introduces the system model, relaying scheme, and the problem formulations. The proposed iterative algorithm for optimizing the compress-and-forward scheme is presented in Section III. Section IV provides interpretations for the optimal structure of quantization noise and characterizes the sensitivity of the achievable rate to changes in the relaying link capacity. Section V provides a DoF analysis of the MIMO relay channel. Section VI interprets the DoF analysis via a connection to deterministic relay channel. Section VII shows that compress-and-forward achieves the capacity of the MIMO Gaussian relay channel with noise correlation to within a constant additive gap. Simulation results are presented in Section VIII, and Section IX concludes the paper.

## II. MIMO GAUSSIAN RELAY CHANNEL WITH NOISE CORRELATION

### A. System Model

Consider the transmission from a BS to a cell-edge user that is located in close proximity of a relay node in a wireless cellular network, as shown in Fig. 1. The relay and the destination observe common interference from nearby BSs and treat it as noise. Due to the common interference, the observed noises across the relay and the destination antennas are correlated. An out-of-band relay link is established between the relay and the user device for interference mitigation and signal enhancement.

Mathematically, this communication scenario is modeled as a Gaussian MIMO relay channel with noise correlation and with a digital relaying link of capacity  $C_0$  bits. The source, relay, and destination are equipped with  $s$ ,  $r$ , and  $d$  antennas, respectively. Let  $t$  be the total number of antennas from all the interfering BSs. The received signals at the relay and the destination can be written as

$$\mathbf{Y}_R = H_{SR}\mathbf{X} + \mathbf{N}_R, \quad (1)$$

$$\mathbf{Y}_D = H_{SD}\mathbf{X} + \mathbf{N}_D, \quad (2)$$

where

$$\mathbf{N}_R = H_{TR}\mathbf{X}_T + \mathbf{N}_1, \quad (3)$$

$$\mathbf{N}_D = H_{TD}\mathbf{X}_T + \mathbf{N}_2 \quad (4)$$

are the correlated noise vectors. Here,  $H_{SR} \in \mathbb{C}^{r \times s}$  and  $H_{SD} \in \mathbb{C}^{d \times s}$  are the source-relay and source-destination channel matrices respectively;  $H_{TR} \in \mathbb{C}^{r \times t}$  and  $H_{TD} \in \mathbb{C}^{d \times t}$  are the interferers-to-relay and interferers-to-destination channel matrices respectively;  $\mathbf{N}_1 \sim \mathcal{CN}(\mathbf{0}_{r \times 1}, \sigma^2 \mathbf{I}_r)$  and  $\mathbf{N}_2 \sim \mathcal{CN}(\mathbf{0}_{d \times 1}, \sigma^2 \mathbf{I}_d)$  are the additive and independent background noises at the relay and the destination respectively;  $\mathbf{X} \in \mathbb{C}^{s \times 1}$  is the transmit signal vector from the source under power constraint  $\mathbb{E}(\mathbf{X}^\dagger \mathbf{X}) \leq P$ ; finally  $\mathbf{X}_T \in \mathbb{C}^{t \times 1}$  is the interference signal vector that is assumed to be Gaussian with  $\mathbf{X}_T \sim \mathcal{CN}(\mathbf{0}_{t \times 1}, S_{\mathbf{X}_T})$ , independent of everything else, and is treated as a part of noise. In order to carry out DoF analysis, we assume that the entries of the channel matrices are drawn independently from a continuous probability distribution, so that each of them as well as their concatenations are full-rank almost surely. Throughout this paper, we assume that the channel state information is known perfectly.

### B. Capacity Upper and Lower Bounds

In this section, we state the cut-set upper bound as well as two expressions for the compress-and-forward lower bound on the capacity of the relay channel. We use these well-known results throughout the paper.

The capacity of the relay channel is upper bounded by [1, Theorem 4]:

$$C \leq \max_{p(\mathbf{x})} \min\{I(\mathbf{X}; \mathbf{Y}_R, \mathbf{Y}_D), I(\mathbf{X}; \mathbf{Y}_D) + C_0\}. \quad (5)$$

$\mathbb{E}\{\mathbf{X}^\dagger \mathbf{X}\} \leq P$

The evaluation of this bound, known as cut-set upper bound, is a convex optimization problem. Here, the optimal  $p(\mathbf{x})$  is a multivariate Gaussian, i.e.,  $\mathbf{X} \sim \mathcal{CN}(\mathbf{0}_{s \times 1}, S_{\mathbf{X}})$  for some positive semidefinite  $S_{\mathbf{X}}$ .

The capacity of the relay channel is lower bounded by [1, Theorem 6]:

$$C \geq \max_{p(\mathbf{x})p(\hat{\mathbf{Y}}_R|\mathbf{Y}_R)} I(\mathbf{X}; \hat{\mathbf{Y}}_R, \mathbf{Y}_D) \quad (6)$$

subject to  $I(\mathbf{Y}_R; \hat{\mathbf{Y}}_R|\mathbf{Y}_D) \leq C_0,$   
 $\mathbb{E}\{\mathbf{X}^\dagger \mathbf{X}\} \leq P.$

The evaluation of this bound, known as the compress-and-forward rate, is not always straightforward. For the Gaussian relay channel, although it can be shown that Gaussian quantization at the relay is optimal for Gaussian signaling at the source [8] and vice versa, the jointly optimal input distribution and quantization test channel of the compress-and-forward lower bound is not yet known; see [17] for an example where jointly Gaussian distribution is suboptimal. For tractability, this paper restricts attention to jointly Gaussian transmission  $\mathbf{X} \sim \mathcal{CN}(\mathbf{0}_{s \times 1}, S_{\mathbf{X}})$  and Gaussian quantization modeled as

$$\hat{\mathbf{Y}}_R = \mathbf{Y}_R + \mathbf{Q}, \quad (7)$$

where the quantization noise  $\mathbf{Q} \sim \mathcal{CN}(\mathbf{0}_{r \times 1}, S_{\mathbf{Q}})$  is independent of all variables. Even then, the optimization of the achievable rate over  $(S_{\mathbf{X}}, S_{\mathbf{Q}})$  is still not straightforward. This optimization is a main subject of this paper.

In the above compress-and-forward scheme, the destination first decodes the quantized version of the relay's observation

uniquely, then proceeds to decode the source message. Reliable unique decoding of the quantization codeword requires the compression rate at the relay not to exceed the relaying link capacity. In an alternative decoding scheme, the destination decodes the message by non-unique decoding of the quantization codeword at the relay, thus allowing the compression rate at the relay to potentially exceed the relay link capacity. Although it can be shown that such a flexibility does not result in a higher achievable rate, the resulting rate expression has the advantage of resembling the cut-set bound, which is useful in characterizing the capacity of the relay channel to within a constant gap. This alternative rate expression is [18, Theorem 16.4]:

$$C \geq \max_{\substack{p(\mathbf{x})p(\hat{\mathbf{y}}_R|\mathbf{y}_R), \\ \mathbb{E}\{\mathbf{X}^\dagger \mathbf{X}\} \leq P}} \min \left\{ I(\mathbf{X}; \hat{\mathbf{Y}}_R, \mathbf{Y}_D), \right. \\ \left. I(\mathbf{X}; \mathbf{Y}_D) + C_0 - I(\mathbf{Y}_R; \hat{\mathbf{Y}}_R | \mathbf{Y}_D, \mathbf{X}) \right\}. \quad (8)$$

Optimization problems (6) and (8) have the same global maximum, and their optimal distributions  $p(\mathbf{x})p(\hat{\mathbf{y}}_R|\mathbf{y}_R)$  are equal.

### C. Problem Formulation

This paper addresses four aspects of MIMO compress-and-forward relaying in the presence of noise correlation.

1) *Optimization of Input and Quantization Covariance Matrices:* We propose a method for optimizing the achievable rate (6). Assuming jointly Gaussian input distribution and quantization test channel, the achievable rate (6) can be expressed as

$$R_{CF}(C_0) = \max_{S_{\mathbf{X}}, S_{\mathbf{Q}}} f_o(S_{\mathbf{X}}, S_{\mathbf{Q}}) \\ \text{subject to } \begin{cases} f_c(S_{\mathbf{X}}, S_{\mathbf{Q}}) \leq C_0, \\ \text{tr}(S_{\mathbf{X}}) \leq P, \\ S_{\mathbf{X}} \succeq \mathbf{0}, S_{\mathbf{Q}} \succeq \mathbf{0}, \end{cases} \quad (9)$$

where the objective function is

$$f_o(S_{\mathbf{X}}, S_{\mathbf{Q}}) = I(\mathbf{X}; \hat{\mathbf{Y}}_R, \mathbf{Y}_D) \\ = \log \frac{\left| HS_{\mathbf{X}}H^\dagger + S_{\text{int}} + \sigma^2 \mathbf{I}_{(r+d)} + \begin{bmatrix} S_{\mathbf{Q}} & \mathbf{0}_{r \times d} \\ \mathbf{0}_{d \times r} & \mathbf{0}_{d \times d} \end{bmatrix} \right|}{\left| S_{\text{int}} + \sigma^2 \mathbf{I}_{(r+d)} + \begin{bmatrix} S_{\mathbf{Q}} & \mathbf{0}_{r \times d} \\ \mathbf{0}_{d \times r} & \mathbf{0}_{d \times d} \end{bmatrix} \right|}, \quad (10)$$

and the constraint is

$$f_c(S_{\mathbf{X}}, S_{\mathbf{Q}}) = I(\mathbf{Y}_R; \hat{\mathbf{Y}}_R | \mathbf{Y}_D) \\ = \log \frac{\left| HS_{\mathbf{X}}H^\dagger + S_{\text{int}} + \sigma^2 \mathbf{I}_{(r+d)} + \begin{bmatrix} S_{\mathbf{Q}} & \mathbf{0}_{r \times d} \\ \mathbf{0}_{d \times r} & \mathbf{0}_{d \times d} \end{bmatrix} \right|}{\left| H_{SD}S_{\mathbf{X}}H_{SD}^\dagger + S_{\text{int}}^{(2,2)} + \sigma^2 \mathbf{I}_d \right| |S_{\mathbf{Q}}|}, \quad (11)$$

where  $H = [H_{SR}^\dagger \ H_{SD}^\dagger]^\dagger$ , and

$$S_{\text{int}} = \begin{bmatrix} S_{\text{int}}^{(1,1)} & S_{\text{int}}^{(1,2)} \\ S_{\text{int}}^{(2,1)} & S_{\text{int}}^{(2,2)} \end{bmatrix} = \begin{bmatrix} H_{TR}S_{\mathbf{X}_t}H_{TR}^\dagger & H_{TR}S_{\mathbf{X}_t}H_{TD}^\dagger \\ H_{TD}S_{\mathbf{X}_t}H_{TR}^\dagger & H_{TD}S_{\mathbf{X}_t}H_{TD}^\dagger \end{bmatrix} \quad (12)$$

is the interference covariance matrix.

2) *Characterization of the Slope of Achievable Rate with Respect to  $C_0$ :* We evaluate the effectiveness of compress-and-forward in improving the overall rate in a relay channel as measured by the slope

$$\frac{d\bar{R}_{CF}(C_0)}{dC_0}, \quad (13)$$

where  $\bar{R}_{CF}(C_0)$  is the achievable rate expression (9) evaluated at a fixed  $S_{\mathbf{X}}$ . We argue that  $\bar{R}_{CF}(C_0)$  is concave in  $C_0$ . Therefore, its maximum slope occurs at  $C_0 = 0$ . By the upper bound (5), this slope cannot exceed 1. This paper provides conditions under which the slope is asymptotically close to its maximum value of 1.

3) *DoF Improvement by Compress-and-Forward:* We also evaluate the effectiveness of compress-and-forward in the large  $C_0$  and high SNR and INR regime by studying the improvement in spatial DoF due to relaying. In particular, define

$$\rho \triangleq \frac{1}{\sigma^2}, \quad (14)$$

and let the relaying link capacity scale with  $\rho$  as

$$C_0(\rho) = \alpha \log(\rho) + o(\log(\rho)). \quad (15)$$

The DoF improvement due to relaying is defined as

$$\Delta \text{DoF} \triangleq \lim_{\rho \rightarrow \infty} \frac{R_{CF}(C_0(\rho)) - R_{CF}(0)}{\log(\rho)}. \quad (16)$$

We show that the conditions on the number of antennas in the system  $(s, d, r, t)$  under which relaying with  $\alpha = \infty$  brings in a DoF improvement are identical to the conditions on the number of antennas under which at small  $C_0$  the slope (13) asymptotically approaches its maximum value.

4) *Characterizing the Capacity to Within a Constant Gap:* Finally, we show the constant-gap optimality of the compress-and-forward strategy for the MIMO relay channel with noise correlation. We bound the gap between the achievable rate (9) and the cut-set bound (5) by a constant that only depends on the number of antennas.

## III. OPTIMIZATION OF COMPRESS-AND-FORWARD

The joint optimization of transmission at the source and quantization at the relay is crucial for efficient use of the relay. This section provides a method for joint optimization of  $S_{\mathbf{X}}$  and  $S_{\mathbf{Q}}$ , and illustrates the structure of  $S_{\mathbf{X}}$  and  $S_{\mathbf{Q}}$  at the stationary point of the overall optimization problem (9).

### A. Iterative Optimization of Lagrangian

The joint optimization of the input and quantization covariance matrices is not a convex optimization problem, as both the objective function and the constraint of (9) are concave in  $S_{\mathbf{X}}$  and convex in  $S_{\mathbf{Q}}$ . Our approach for tackling (9) is to first find a stationary point of the Lagrangian

$$\mathcal{L}(S_{\mathbf{X}}, S_{\mathbf{Q}}, \mu) = f_o(S_{\mathbf{X}}, S_{\mathbf{Q}}) - \mu(f_c(S_{\mathbf{X}}, S_{\mathbf{Q}}) - C_0), \quad (17)$$

**Algorithm 1** Joint Input and Quantization Optimization (9)

- 
- 1: Initialize  $S_{\mathbf{X}} \succeq \mathbf{0}$  such that  $\text{tr}(S_{\mathbf{X}}) = P$ ;
  - 2: **repeat**
  - 3:   For a fixed  $\mu$ :
  - 4:   **repeat**
  - 5:     Find optimal  $S_{\mathbf{Q}}$  for fixed  $S_{\mathbf{X}}$  as in Section III-C;
  - 6:     Find optimal  $S_{\mathbf{X}}$  for fixed  $S_{\mathbf{Q}}$  as in Section III-B;
  - 7:   **until** Convergence;
  - 8:   Update  $\mu$  using bisection;
  - 9: **until**  $f_c(S_{\mathbf{X}}, S_{\mathbf{Q}}) = C_0$ .
- 

for a fixed Lagrange multiplier  $\mu$  by solving

$$\begin{aligned} & \underset{S_{\mathbf{X}}, S_{\mathbf{Q}}}{\text{maximize}} && \mathcal{L}(S_{\mathbf{X}}, S_{\mathbf{Q}}, \mu) \\ & \text{subject to} && \text{tr}(S_{\mathbf{X}}) \leq P, \\ & && S_{\mathbf{X}} \succeq \mathbf{0}, S_{\mathbf{Q}} \succeq \mathbf{0}, \end{aligned} \quad (18)$$

then to search for the  $\mu$  that results in

$$f_c(S_{\mathbf{X}}^*, S_{\mathbf{Q}}^*) = C_0, \quad (19)$$

in an outer loop. It can be easily shown that the optimal  $\mu^* \in (0, 1)$ , because if  $\mu \geq 1$ , i.e., if the relay link capacity constraint penalizes the objective at more than a 1:1 ratio, then the optimal  $S_{\mathbf{Q}}^*$  would be infinite, resulting in  $f_c(S_{\mathbf{X}}, S_{\mathbf{Q}}^*) = 0$ . Thus, finding  $\mu^*$  is a one-dimensional root-finding problem. If  $f_c(S_{\mathbf{X}}^*(\mu), S_{\mathbf{Q}}^*(\mu))$  is continuous in  $\mu \in (0, 1)$ , then the optimal  $\mu$  that satisfies (19) can be found by bisection. In case of discontinuity, time-sharing between the two operating points is needed.

We propose an iterative coordinate ascent approach for solving (18). In an iteration of this coordinate ascent procedure, we obtain the global optimum of  $S_{\mathbf{X}}$  and  $S_{\mathbf{Q}}$  while keeping the other variable fixed (and the global optimum is essentially unique). This iteration process generates a nondecreasing sequence of the Lagrangian objective values; hence, it converges.

Details of optimizing  $S_{\mathbf{Q}}$  for a fixed  $S_{\mathbf{X}}$  and optimizing  $S_{\mathbf{X}}$  for a fixed  $S_{\mathbf{Q}}$  are provided in the subsequent sections. The overall iterative approach is summarized as Algorithm 1. The following theorem states the convergence result formally.

*Theorem 1:* Assuming that the optimal  $S_{\mathbf{X}}$  for a fixed  $S_{\mathbf{Q}}$  is unique and the optimal  $S_{\mathbf{Q}}$  for a fixed  $S_{\mathbf{X}}$  is unique, the inner iterative optimization procedure in Algorithm 1 converges to a stationary point of the Lagrangian maximization problem (18). Further, if bisection finds the  $\mu$  that satisfies (19), then such a  $\mu$  leads to a Karush-Kuhn-Tucker (KKT) point of the joint transmit and quantization noise covariance optimization problem (9).

*Proof:* For a fixed  $\mu$ , coordinate ascent on the Lagrangian is monotonically increasing; hence, it is convergent. The uniqueness of solution in the optimization of  $S_{\mathbf{X}}$  for a fixed  $S_{\mathbf{Q}}$  and in the optimization of  $S_{\mathbf{Q}}$  for a fixed  $S_{\mathbf{X}}$  ensures that coordinate ascent converges to a stationary point. This together with  $\mu$  that satisfies (19) gives a KKT point of (9). ■

There are special cases, for example when  $s = 1$  or  $r = 1$ , where the above procedure would produce a globally optimal solution. However, in general only the convergence to a stationary point is assured.

**B. Optimization of  $S_{\mathbf{X}}$  for a Fixed  $S_{\mathbf{Q}}$** 

Although the optimization problem (9) is not concave in  $S_{\mathbf{X}}$  for fixed  $S_{\mathbf{Q}}$ , we observe that the maximization of its Lagrangian (17) at a given  $\bar{S}_{\mathbf{Q}}$  is concave for fixed  $\mu \in (0, 1)$ . Therefore, solving the maximization

$$\begin{aligned} & \underset{S_{\mathbf{X}}}{\text{maximize}} && \mathcal{L}(S_{\mathbf{X}}, \bar{S}_{\mathbf{Q}}, \mu) \\ & \text{subject to} && \text{tr}(S_{\mathbf{X}}) \leq P, \\ & && S_{\mathbf{X}} \succeq \mathbf{0}, \end{aligned} \quad (20)$$

using standard tools from convex optimization provides a global optimum of  $S_{\mathbf{Q}}$  for the fixed  $S_{\mathbf{X}}$ ; see the general sufficiency [19, Proposition 3.3.4]. To verify concavity, note that for fixed  $S_{\mathbf{Q}}$  the Lagrangian can be written as a function of  $S_{\mathbf{X}}$  as

$$\begin{aligned} & \mathcal{L}(S_{\mathbf{X}}, \bar{S}_{\mathbf{Q}}, \mu) \\ & = I(\mathbf{X}; \hat{\mathbf{Y}}_R, \mathbf{Y}_D) - \mu I(\mathbf{Y}_R; \hat{\mathbf{Y}}_R | \mathbf{Y}_D) + \mu C_0 \\ & = (1 - \mu) I(\mathbf{X}; \hat{\mathbf{Y}}_R, \mathbf{Y}_D) + \mu I(\mathbf{X}; \mathbf{Y}_D) + \text{const.} \\ & = (1 - \mu) \log \left| H S_{\mathbf{X}} H^\dagger + S_{\text{int}} + \sigma^2 \mathbf{I}_{(r+d)} + \begin{bmatrix} \bar{S}_{\mathbf{Q}} & \mathbf{0}_{r \times d} \\ \mathbf{0}_{d \times r} & \mathbf{0}_{d \times d} \end{bmatrix} \right| \\ & \quad + \mu \log \left| H_{SD} S_{\mathbf{X}} H_{SD}^\dagger + S_{\text{int}}^{(2,2)} + \sigma^2 \mathbf{I}_d \right| + \text{const.}, \end{aligned} \quad (21)$$

which is a concave logdet function for  $\mu \in (0, 1)$ .

The above form of the Lagrangian provides intuition about the optimal choice of  $S_{\mathbf{X}}$ . The Lagrangian is a convex combination of two terms. The first term corresponds to the channel from  $\mathbf{X}$  to the combined relay and destination receiver  $(\hat{\mathbf{Y}}_R, \mathbf{Y}_D)$ , while the second term corresponds to the channel from  $\mathbf{X}$  to the destination  $\mathbf{Y}_D$  alone. For larger values of  $C_0$  (or equivalently small values of  $\mu$ ), the optimal  $S_{\mathbf{X}}$  should be close to the water-filling covariance matrix against the combined vector channel  $H$ . For small values of  $C_0$ , the optimal  $S_{\mathbf{X}}$  should be close to the water-filling covariance matrix against the source-destination channel  $H_{SD}$  alone. For a finite  $C_0$ , the optimal beamforming is obtained by maximizing the convex combination of the two terms.

**C. Optimization of  $S_{\mathbf{Q}}$  for a Fixed  $S_{\mathbf{X}}$** 

We now provide a closed-form solution for the  $S_{\mathbf{Q}}$  that maximizes the Lagrangian (18) for a given  $\bar{S}_{\mathbf{X}}$ , i.e., the solution of

$$\begin{aligned} & \underset{S_{\mathbf{Q}}}{\text{maximize}} && \mathcal{L}(\bar{S}_{\mathbf{X}}, S_{\mathbf{Q}}, \mu) \\ & \text{subject to} && S_{\mathbf{Q}} \succeq \mathbf{0}. \end{aligned} \quad (22)$$

For the optimization of  $S_{\mathbf{Q}}$  when  $\bar{S}_{\mathbf{X}}$  is kept fixed, the objective and constraint functions (10)-(11) can be rewritten as

$$f_o = \log |S_{\mathbf{Y}_R | \mathbf{Y}_D} + S_{\mathbf{Q}}| - \log |S_{\mathbf{Y}_R | \mathbf{Y}_D, \mathbf{X}} + S_{\mathbf{Q}}| + \text{const.}, \quad (23)$$

$$f_c = \log |S_{\mathbf{Y}_R | \mathbf{Y}_D} + S_{\mathbf{Q}}| - \log |S_{\mathbf{Q}}| + \text{const.}, \quad (24)$$

and Lagrangian in (22) can be rewritten as

$$\begin{aligned} \mathcal{L}(\bar{S}_{\mathbf{X}}, S_{\mathbf{Q}}, \mu) & = (1 - \mu) \log |S_{\mathbf{Y}_R | \mathbf{Y}_D} + S_{\mathbf{Q}}| + \mu \log |S_{\mathbf{Q}}| \\ & \quad - \log |S_{\mathbf{Y}_R | \mathbf{Y}_D, \mathbf{X}} + S_{\mathbf{Q}}| + \text{const.}, \end{aligned} \quad (25)$$

where the conditional covariances are obtained using the generalized Schur complement formula [20]

$$\begin{aligned} S_{\mathbf{Y}_R|\mathbf{Y}_D} &= H_{SR}S_{\mathbf{X}}H_{SR}^\dagger + S_{\text{int}}^{(1,1)} + \sigma^2\mathbf{I}_r - (H_{SR}S_{\mathbf{X}}H_{SD}^\dagger + S_{\text{int}}^{(1,2)}) \\ & (H_{SD}S_{\mathbf{X}}H_{SD}^\dagger + S_{\text{int}}^{(2,2)} + \sigma^2\mathbf{I}_d)^{-1} (H_{SD}S_{\mathbf{X}}H_{SR}^\dagger + S_{\text{int}}^{(2,1)}), \end{aligned} \quad (26)$$

and

$$\begin{aligned} S_{\mathbf{Y}_R|\mathbf{Y}_D,\mathbf{X}} &= H_{SR}S_{\mathbf{X}}H_{SR}^\dagger + S_{\text{int}}^{(1,1)} + \sigma^2\mathbf{I}_r \\ & - [H_{SR}S_{\mathbf{X}}H_{SD}^\dagger + S_{\text{int}}^{(1,2)} \quad H_{SR}S_{\mathbf{X}}] \\ & \cdot \begin{bmatrix} H_{SD}S_{\mathbf{X}}H_{SD}^\dagger + S_{\text{int}}^{(2,2)} + \sigma^2\mathbf{I}_d & H_{SD}S_{\mathbf{X}} \\ S_{\mathbf{X}}H_{SD}^\dagger & S_{\mathbf{X}} \end{bmatrix}^{-1} \\ & \cdot \begin{bmatrix} H_{SD}S_{\mathbf{X}}H_{SR}^\dagger + S_{\text{int}}^{(2,1)} \\ S_{\mathbf{X}}H_{SR}^\dagger \end{bmatrix}. \end{aligned} \quad (27)$$

The main step in obtaining the global optimum of (25) in closed form is the following simultaneous diagonalization by \*congruence of  $S_{\mathbf{Y}_R|\mathbf{Y}_D,\mathbf{X}}$  and  $S_{\mathbf{Y}_R|\mathbf{Y}_D}$  based on [6, Corollary 7.6.5].

*Lemma 1:* There exists a non-singular matrix  $C_R \in \mathbb{C}^{r \times r}$  such that  $C_R^\dagger S_{\mathbf{Y}_R|\mathbf{Y}_D,\mathbf{X}} C_R = \mathbf{I}_r$  and  $C_R^\dagger S_{\mathbf{Y}_R|\mathbf{Y}_D} C_R = \Lambda$ , where  $\Lambda$  is a diagonal matrix. The diagonal elements  $\lambda_i$ 's are called the generalized eigenvalues, and we have  $\lambda_i \geq 1$  for  $i = 1, \dots, r$ .

*Proof:* Both  $S_{\mathbf{Y}_R|\mathbf{Y}_D}$  and  $S_{\mathbf{Y}_R|\mathbf{Y}_D,\mathbf{X}}$  are positive definite matrices. Let  $S_{\mathbf{Y}_R|\mathbf{Y}_D,\mathbf{X}}^{-1} = R^\dagger R$  be the Cholesky decomposition. Now, consider the eigendecomposition  $R S_{\mathbf{Y}_R|\mathbf{Y}_D} R^\dagger = V \Lambda V^\dagger$ . Then  $C_R = R^\dagger V$  satisfies  $C_R^\dagger S_{\mathbf{Y}_R|\mathbf{Y}_D,\mathbf{X}} C_R = \mathbf{I}_r$  and  $C_R^\dagger S_{\mathbf{Y}_R|\mathbf{Y}_D} C_R = \Lambda$  simultaneously. Moreover,  $S_{\mathbf{Y}_R|\mathbf{Y}_D} \succeq S_{\mathbf{Y}_R|\mathbf{Y}_D,\mathbf{X}}$  implies  $\Lambda \succeq \mathbf{I}_r$ . ■

The above transformation makes elements of the relay's observed vector conditionally independent. We can now use the approach of [4], [21] to solve the quantization noise optimization problem for describing the independent elements. For  $\mu \in (0, 1)$ , the Lagrangian (25) can be written as

$$\begin{aligned} \mathcal{L} &\stackrel{(a)}{=} (1 - \mu) \log \left| \Lambda \hat{S}_{\mathbf{Q}}^{-1} + \mathbf{I}_r \right| - \log \left| \hat{S}_{\mathbf{Q}}^{-1} + \mathbf{I}_r \right| + \text{const.} \\ &\stackrel{(b)}{\leq} (1 - \mu) \log \left| \Lambda \Sigma_{\mathbf{Q}}^{-1} + \mathbf{I}_r \right| - \log \left| \Sigma_{\mathbf{Q}}^{-1} + \mathbf{I}_r \right| + \text{const.} \end{aligned} \quad (28)$$

where (a) follows from the change of variable  $\hat{S}_{\mathbf{Q}} = C_R^\dagger S_{\mathbf{Q}} C_R$ , with  $C_R$  as in Lemma 1, and (b) follows from [21, Lemma 5] where  $\Sigma_{\mathbf{Q}}$  comes from the eigendecomposition  $\hat{S}_{\mathbf{Q}} = U \Sigma_{\mathbf{Q}} U^\dagger$ . Observe that the equality in (b) is obtained with  $U = \mathbf{I}_r$ . Thus, it is without loss of optimality to restrict  $\hat{S}_{\mathbf{Q}}$  to be diagonal.

Consider the change of variable [4]

$$c_i = \log \left( 1 + \frac{\lambda_i}{\Sigma_{\mathbf{Q}}^{ii}} \right), \quad i = 1, \dots, r, \quad (29)$$

where  $\Sigma_{\mathbf{Q}}^{ii}$ 's are the diagonal entries of  $\Sigma_{\mathbf{Q}}$ . An interpretation of  $c_i$  is that it is the portion of the available  $C_0$  allocated

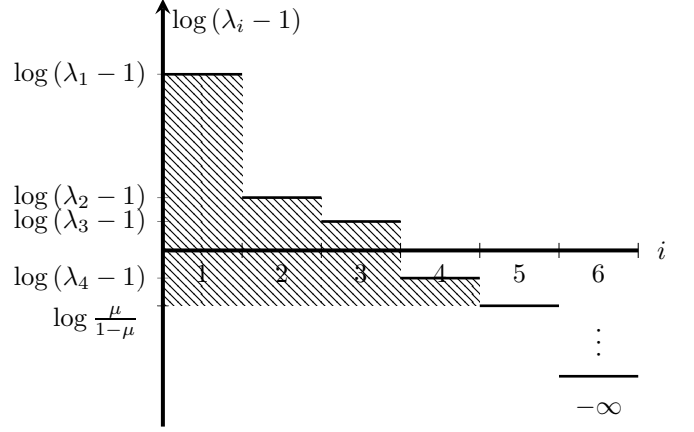


Fig. 2. Reverse water-filling for allocating  $C_0$  among elements of  $C_R \mathbf{Y}_R$  when  $C_0 = \bar{C}_{0,5}$ . The first component is asymptotically deterministic and the 6<sup>th</sup> component is reversely degraded. This happens, e.g., when  $(s, d, r, t) = (5, 2, 6, 7)$ .

for quantization of the  $i^{\text{th}}$  element of  $C_R \mathbf{Y}_R$ . Using (29), the Lagrangian can be written as

$$\mathcal{L} = \sum_{i=1}^r ((1 - \mu) c_i - \log(2^{c_i} + \lambda_i - 1)) + \text{const.} \quad (30)$$

It can be readily checked that (30) is concave in  $c_i$  for  $\lambda_i \geq 1$ . It is easy to see that the optimal  $c_i^*$  is

$$c_i^* = \left[ \log(\lambda_i - 1) - \log \frac{\mu}{1 - \mu} \right]^+, \quad (31)$$

therefore,  $\Sigma_{\mathbf{Q}}^{ii,*}$  is given by

$$\Sigma_{\mathbf{Q}}^{ii,*} = \begin{cases} \frac{\mu}{1 - \frac{\mu}{\lambda_i} - \mu} & \mu < 1 - \frac{1}{\lambda_i} \\ +\infty & \mu \geq 1 - \frac{1}{\lambda_i} \end{cases}. \quad (32)$$

The optimal  $S_{\mathbf{Q}}$  is  $S_{\mathbf{Q}}^* = C_R^{-\dagger} \Sigma_{\mathbf{Q}}^* C_R^{-1}$ .

The above solution illustrates that the optimal compression involves independent quantization of elements of the relay's observed vector after transformation by matrix  $C_R$  at quantization rates given by (31). This solution allocates quantization rates to elements of  $C_R \mathbf{Y}_R$  using reverse water-filling on  $\log(\lambda_i - 1)$ 's. An example of such a reverse water-filling rate allocation is shown in Fig. 2. Here,  $\lambda_i - 1$  can be thought of as the  $i^{\text{th}}$  element's CSINR given  $\mathbf{Y}_D$ . To illustrate this interpretation of CSINR through an example, consider the case of  $r = 1$ , where we have

$$\lambda_1 - 1 = \frac{S_{\mathbf{Y}_R|\mathbf{Y}_D} - S_{\mathbf{Y}_R|\mathbf{Y}_D,\mathbf{X}}}{S_{\mathbf{Y}_R|\mathbf{Y}_D,\mathbf{X}}}. \quad (33)$$

This is the ratio of the conditional variance of signal to the conditional variance of interference plus noise given  $\mathbf{Y}_D$ . In the next section, we explain how the magnitude of generalized eigenvalues determines the performance of MIMO compress-and-forward relaying.

A special case of this optimization problem is considered in [4], where the noises at  $\mathbf{Y}_R$  and  $\mathbf{Y}_D$  are independent and  $S_{\mathbf{Y}_R|\mathbf{Y}_D,\mathbf{X}}$  is an identity matrix. In this case  $S_{\mathbf{Y}_R|\mathbf{Y}_D,\mathbf{X}}$  and  $S_{\mathbf{Y}_R|\mathbf{Y}_D}$  can be diagonalized simultaneously by the CKLT of

$\mathbf{Y}_R$  given  $\mathbf{Y}_D$ , which is a unitary transformation [5]. For the more general correlated noise case, the above simultaneous diagonalization is needed to transform the matrix optimization problem to scalar optimization.

We note that in [8] a diagonalization approach, known as CCA, is used to solve the same problem, but from a source coding perspective. Instead of diagonalizing  $S_{\mathbf{Y}_R|\mathbf{Y}_D,\mathbf{X}}$  and  $S_{\mathbf{Y}_R|\mathbf{Y}_D}$ , the approach of [8] diagonalizes  $S_{\mathbf{X}|\mathbf{Y}_D}$  and  $S_{\mathbf{Y}_R|\mathbf{Y}_D}$  using a singular value decomposition of the matrix  $S_{\mathbf{X}|\mathbf{Y}_D}^{-1/2} K_{\mathbf{X}\mathbf{Y}_R} S_{\mathbf{Y}_R|\mathbf{Y}_D}^{1/2}$ , where  $K_{\mathbf{X}\mathbf{Y}_R}$  is a certain matrix of regression coefficients. It can be shown that the resulting diagonalization makes  $S_{\mathbf{X}\mathbf{Y}_R|\mathbf{Y}_D}^{(1,2)}$  diagonal as well. Subsequently, the diagonal elements from the diagonalization of  $S_{\mathbf{X}\mathbf{Y}_R|\mathbf{Y}_D}^{(1,2)}$  are used to find the optimal solution to the overall problem. We observe that the CCA approach in [8] can be interpreted as an indirect simultaneous diagonalization of  $S_{\mathbf{Y}_R|\mathbf{Y}_D,\mathbf{X}}$  and  $S_{\mathbf{Y}_R|\mathbf{Y}_D}$ , and is in fact equivalent to the transformation presented here. However, the direct simultaneous diagonalization of  $S_{\mathbf{Y}_R|\mathbf{Y}_D,\mathbf{X}}$  and  $S_{\mathbf{Y}_R|\mathbf{Y}_D}$  is simpler and gives structural insight into the optimal MIMO compress-and-forward strategy.

#### IV. INTERPRETING THE GENERALIZED EIGENVALUES

The optimization of quantization covariance in vector compress-and-forward involves reverse water-filling on  $\log(\lambda_i - 1)$ 's, where  $\lambda_i - 1$  can be interpreted as the CSINR at the  $i^{\text{th}}$  element of  $C_R \mathbf{Y}_R$ . The reverse water-filling solution with respect to CSINRs reveals insight into the effectiveness of MIMO compress-and-forward relaying for improving the achievable rate.

##### A. The Slope of $\bar{R}_{CF}(C_0)$

For the MIMO relay channel under study, the following result relates the slope of  $\bar{R}_{CF}(C_0)$  to the magnitude of the generalized eigenvalues  $\lambda_i$ 's.

*Lemma 2:* In the optimal allocation of the relaying link capacity  $C_0$  to elements of  $C_R \mathbf{Y}_R$  for quantization, given in (31), let  $\bar{C}_{0,i}$  be the largest  $C_0$  for which the optimal quantization rate of the  $i^{\text{th}}$  element is zero, i.e.,  $c_i^* > 0$  if and only if  $C_0 > \bar{C}_{0,i}$ . We have

$$\bar{C}_{0,i} = \sum_{j=1}^{i-1} \log \frac{\lambda_j - 1}{\lambda_i - 1}, \quad i = 2, \dots, r, \quad (34)$$

and

$$\left. \frac{d\bar{R}_{CF}(C_0)}{dC_0} \right|_{C_0=\bar{C}_{0,i}} = 1 - \frac{1}{\lambda_i}, \quad (35)$$

where  $\bar{R}_{CF}(C_0)$  is (9) evaluated at given  $\bar{S}_{\mathbf{X}}$ .

*Proof:* By the result of Section III-C, the optimization problem (22) can be transformed into a convex problem, therefore strong duality holds. Moreover, the optimized  $\bar{R}_{CF}(C_0)$  is differentiable over  $C_0 > 0$ . The slope of  $\bar{R}_{CF}(C_0)$  is in fact the optimal Lagrange multiplier in the KKT solution at the given  $C_0$  [22], i.e.,

$$\frac{d\bar{R}_{CF}(C_0)}{dC_0} = \mu^*(C_0). \quad (36)$$

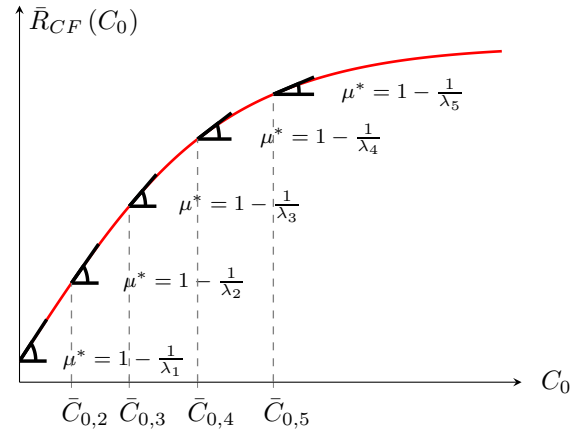


Fig. 3. For a fixed  $\bar{S}_{\mathbf{X}}$ , the slope of the optimized compress-and-forward rate curve at  $\bar{C}_{0,i}$  is  $1 - \frac{1}{\lambda_i}$  for  $i = 1, \dots, r$ .

When  $C_0$  is such that  $c_i^* = 0$  and  $c_1^* + \dots + c_{i-1}^* = C_0$  for  $2 \leq i \leq r$ , using the KKT solution (31), the Lagrange multiplier is given by

$$\mu^*(C_0) = \frac{1}{1 + \left( \frac{2C_0}{\prod_{j=1}^{i-1} (\lambda_j - 1)} \right)^{\frac{1}{i-1}}}. \quad (37)$$

Now,  $\bar{C}_{0,i}$  is the largest value of  $C_0$  for which the optimal quantization rate of the  $i^{\text{th}}$  element is zero,  $c_i^* = 0$ . Using (31) again, we have

$$\log \frac{1 - \mu^*(\bar{C}_{0,i})}{\mu^*(\bar{C}_{0,i})} + \log(\lambda_i - 1) = 0. \quad (38)$$

This together with (36) and (37) yields (34) and (35). ■

Fig. 3 illustrates this result. The slope of the compress-and-forward achievable rate at various points of  $C_0$  is determined by the generalized eigenvalues of the conditional covariance matrices. A larger  $\lambda_i$  implies a slope closer to the maximum value of 1.

##### B. Zero CSINR: Reversely Degraded Components

When  $\lambda_i(S_{\mathbf{Y}_R|\mathbf{Y}_D} S_{\mathbf{Y}_R|\mathbf{Y}_D,\mathbf{X}}^{-1}) = 1$ , the corresponding element in  $C_R \mathbf{Y}_R$  is conditionally independent of  $\mathbf{X}$  given  $\mathbf{Y}_D$ . Since such an element does not convey any further information to destination, the optimized compress-and-forward does not assign any portion of  $C_0$  for describing it.

*Definition 1:* The  $i^{\text{th}}$  element of  $C_R \mathbf{Y}_R$  is called reversely degraded, if  $\lambda_i(S_{\mathbf{Y}_R|\mathbf{Y}_D} S_{\mathbf{Y}_R|\mathbf{Y}_D,\mathbf{X}}^{-1}) = 1$ .

When the relay node is equipped with a large number of antennas, the number of elements of  $C_R \mathbf{Y}_R$  to be quantized, i.e., the elements that are not reversely degraded, can be much smaller than the number of relay antennas. The following proposition bounds the number of reversely degraded components in the relay channel. It shows that the optimal scheme quantizes no more than  $\min(r, s^r)$  elements. This result is used for the constant gap characterization of the capacity in Section VII as well.

*Theorem 2:* In the MIMO relay channel under study, the number of reversely degraded components is at least  $(r - s^r)^+$ ,

where  $s^r$  is the number of independent data streams transmitted by the source, i.e.,  $\text{rank}(\bar{S}_{\mathbf{X}}) = s^r$ . Hence, the optimal quantization scheme in (31) describes at most  $\min(r, s^r)$  elements of  $C_R \mathbf{Y}_R$ .

*Proof:* By Lemma 1,  $C_R (S_{\mathbf{Y}_R|\mathbf{Y}_D} - S_{\mathbf{Y}_R|\mathbf{Y}_D, \mathbf{X}}) C_R^\dagger = \Lambda - \mathbf{I}_r$ . Therefore, the number of reversely degraded components of the channel is equal to  $r - \text{rank}(C_R (S_{\mathbf{Y}_R|\mathbf{Y}_D} - S_{\mathbf{Y}_R|\mathbf{Y}_D, \mathbf{X}}) C_R^\dagger) = r - \text{rank}(S_{\mathbf{Y}_R|\mathbf{Y}_D} - S_{\mathbf{Y}_R|\mathbf{Y}_D, \mathbf{X}})$ . Now, using the generalized Schur complement formula, we have

$$S_{\mathbf{Y}_R|\mathbf{Y}_D} - S_{\mathbf{Y}_R|\mathbf{Y}_D, \mathbf{X}} = S_{\mathbf{Y}_R, \mathbf{X}|\mathbf{Y}_D}^{(1,2)} S_{\mathbf{X}|\mathbf{Y}_D}^{-1} S_{\mathbf{Y}_R, \mathbf{X}|\mathbf{Y}_D}^{(2,1)}. \quad (39)$$

The result follows by noting that  $\text{rank}(S_{\mathbf{Y}_R|\mathbf{Y}_D} - S_{\mathbf{Y}_R|\mathbf{Y}_D, \mathbf{X}}) \leq \min(r, s^r)$ . ■

### C. Infinite CSINR: Asymptotically Deterministic Components

Relaying can be particularly effective if the relay observation  $\mathbf{Y}_R$  is a deterministic function of  $(\mathbf{Y}_D, \mathbf{X})$ . For example, this can happen asymptotically in a SISO relay channel with  $(s, d, r, t) = (1, 1, 1, 1)$ , where we have

$$\mathbf{Y}_R = \left( h_{SR} - \frac{h_{TR}h_{SD}}{h_{TD}} \right) \mathbf{X} + \frac{h_{TR}}{h_{TD}} \mathbf{Y}_D + \mathbf{N}_1 - \frac{h_{TR}}{h_{TD}} \mathbf{N}_2, \quad (40)$$

assuming  $h_{TD} \neq 0$  and  $h_{SR}h_{TD} \neq h_{SD}h_{TR}$ . When the noise power is zero, we have  $\mathbf{Y}_R = f(\mathbf{X}, \mathbf{Y}_D)$ . In a relay channel with this type of determinism, compress-and-forward achieves the cut-set upper bound [15], and every relay bit improves the overall transmission rate by exactly one bit (if the relaying link capacity is not too large). In the above example, as  $\sigma^2 \rightarrow 0$ , the slope of  $\bar{R}_{CF}(C_0)$  at small  $C_0$  asymptotically approaches 1; this can be verified by noting that

$$\lim_{\sigma^2 \rightarrow 0} S_{\mathbf{Y}_R|\mathbf{Y}_D} = \frac{|h_{SR}h_{TD} - h_{SD}h_{TR}|^2 P}{|h_{SD}|^2 + |h_{TD}|^2}. \quad (41)$$

and

$$\lim_{\sigma^2 \rightarrow 0} S_{\mathbf{Y}_R|\mathbf{Y}_D, \mathbf{X}} = 0. \quad (42)$$

Thus,  $\lim_{\sigma^2 \rightarrow 0} \lambda_1 = \infty$ . Hence,  $\lim_{\sigma^2 \rightarrow 0} \frac{d\bar{R}_{CF}(C_0)}{dC_0} \Big|_{C_0=0} = 1$  by Lemma 2. The following result reveals the number of asymptotic deterministic components of this type for the MIMO relay channel under consideration.

*Definition 2:* The  $i^{\text{th}}$  element of  $C_R \mathbf{Y}_R$  is called asymptotically deterministic, if  $\lim_{\sigma^2 \rightarrow 0} \lambda_i(S_{\mathbf{Y}_R|\mathbf{Y}_D} S_{\mathbf{Y}_R|\mathbf{Y}_D, \mathbf{X}}^{-1}) = \infty$ .

*Theorem 3:* In the MIMO relay channel under study, the number of asymptotically deterministic components is

$$r' - r'' = \min(r, s^r, (r + d - t)^+, (s^r + t - d)^+), \quad (43)$$

almost surely, where

$$r' \triangleq \text{rank}(S_{\bar{\mathbf{Y}}_R|\bar{\mathbf{Y}}_D}) = \min(r, (s^r + t - d)^+), \quad (44)$$

$$r'' \triangleq \text{rank}(S_{\bar{\mathbf{Y}}_R|\bar{\mathbf{Y}}_D, \mathbf{X}}) = \min(r, (t - d)^+). \quad (45)$$

Here,

$$\bar{\mathbf{Y}}_R \triangleq H_{SR}\mathbf{X} + H_{TR}\mathbf{X}_t, \quad (46)$$

$$\bar{\mathbf{Y}}_D \triangleq H_{SD}\mathbf{X} + H_{TD}\mathbf{X}_t, \quad (47)$$

are the noiseless parts of the relay and destination's observations, respectively. Hence, for  $i = 1, \dots, r' - r''$ , the slope (35) approaches 1 as  $\sigma^2 \rightarrow 0$ .

*Proof:* See Appendix B. ■

A key implication of the above result is the following. For the MIMO relay channel under consideration, relaying with small  $C_0$  is most effective if  $\frac{d\bar{R}_{CF}(C_0)}{dC_0} \Big|_{C_0=0}$  is at the maximum value of 1. This happens when  $\lambda_1 \rightarrow \infty$ , i.e., when the MIMO relay channel has at least one asymptotic deterministic component, or equivalently, by Theorem 3, when  $r' > r''$ . By (43), this holds when  $r + d > t$  and  $d < s^r + t$ . We state this result below and will return to the interpretation of this condition in Section VI.

*Corollary 1:* For the MIMO relay channel under study,  $\lim_{\sigma^2 \rightarrow 0} \frac{d\bar{R}_{CF}(C_0)}{dC_0} \Big|_{C_0=0} = 1$  if and only if  $r + d > t$  and  $d < s^r + t$ .

## V. DOF IMPROVEMENT BY RELAYING

We gain further insight into the benefit of relaying by analyzing DoF of the MIMO relay channel. Consider the DoF of the channel under study without the relay, and with a relay that has infinite link capacity, i.e., respectively,

$$DoF_D \triangleq \lim_{\rho \rightarrow \infty} \frac{R_{CF}(0)}{\log \rho} = \min(s, (d - t)^+), \quad (48)$$

$$DoF_R \triangleq \lim_{\rho \rightarrow \infty} \frac{R_{CF}(\infty)}{\log \rho} = \min(s, (r + d - t)^+). \quad (49)$$

At infinite relay link capacity, the DoF gain due to relaying is

$$DoF_R - DoF_D = \min(r, s, (r + d - t)^+, (s + t - d)^+). \quad (50)$$

Curiously, the above expression is identical to the number of asymptotically deterministic components derived in the previous section. We will return to this connection in the next section.

We now characterize the overall DoF gain due to relaying. First, we note that the design of the combining matrix at the relay is crucial for achieving the optimal DoF. Without any combining, naive i.i.d. quantization of the relay's observed vector on a per-antenna basis results in a DoF loss in general.

*Theorem 4:* For the relay channel under study, the achievable DoF improvement by compress-and-forward with relay's quantization scheme (7) restricted to  $\mathbf{Q} \sim \mathcal{CN}(\mathbf{0}_{r \times 1}, q\mathbf{I}_r)$  is

$$\Delta DoF_{i.i.d.} = (DoF_R - DoF_D) \min\left(1, \frac{\alpha}{r'}\right) \quad (51)$$

almost surely, where  $r' = \text{rank}(S_{\bar{\mathbf{Y}}_R|\bar{\mathbf{Y}}_D}) = \min(r, (s + t - d)^+)$  and  $\alpha$  is the DoF of the relaying link capacity  $C_0$  as in (15).

*Proof:* See Appendix C. ■

Note that when  $d < t$ , the coefficient of  $\alpha$  in (51) is

$$\frac{(DoF_R - DoF_D)}{r'} = \frac{\min(s, r + d - t)}{\min(r, s + t - d)} < 1, \quad (52)$$

whereas, by the next theorem, the coefficient of  $\alpha$  in the optimal DoF gain is 1. This loss in DoF is due to the non-optimized choice of quantization scheme.

The optimal DoF can be achieved by using a combining matrix  $\tilde{C}_R$  of dimension  $\min(r, s, (r+d-t)^+) \times r$  followed by i.i.d. quantization at the relay. The combining matrix aligns the observed interference at the relay with the row space of the observed interference at the destination. The optimality of this scheme follows by the cut-set bound (5). Details of the proof are deferred to Appendix D. We call this combining strategy distributed zero-forcing, because in zero-forcing of interference with  $r+d$  antennas pooled together, the combining matrix  $\tilde{C}_R$  is the submatrix corresponding to  $r$  antennas of the relay.

*Theorem 5:* For the relay channel under study, the optimal DoF improvement by relaying is

$$\Delta DoF^* = \min(DoF_R - DoF_D, \alpha) \quad (53)$$

almost surely.

*Proof:* See Appendix D. ■

## VI. CONNECTION BETWEEN DOF IMPROVEMENT AND ASYMPTOTICALLY DETERMINISTIC COMPONENTS

Combining the results of the previous two sections, we see that the DoF improvement at infinite relay link rate is equal to the number of asymptotically deterministic components in the MIMO relay channel. Thus, the DoF improvement at  $C_0 = \infty$  is related to the slope of the achievable rate at small  $C_0$ . In this section, we first provide an information theoretical proof of this equivalence, then further explore this connection via the DoF-optimal distributed zero-forcing combiner design at the relay.

*Theorem 6:* For the MIMO relay channel under study, the maximum DoF improvement achieved with an infinite capacity relay link is equal to the number of asymptotically deterministic components, i.e.,

$$DoF_R - DoF_D = r' - r''. \quad (54)$$

The DoF gain, or equivalently the number of asymptotically deterministic components, is greater than zero if and only if  $d < s + t$  and  $r + d > t$ .

*Proof:* Fix  $S_{\mathbf{X}}$  to be full-rank. By Theorem 3, the number of asymptotically deterministic components is  $r' - r''$ , the difference of ranks of  $S_{\tilde{\mathbf{Y}}_R|\tilde{\mathbf{Y}}_D}$  and  $S_{\tilde{\mathbf{Y}}_R|\tilde{\mathbf{Y}}_D, \mathbf{X}}$ . To relate this to  $DoF_R - DoF_D$ , we expand the conditional mutual information below in two different ways

$$I(\mathbf{X}; \mathbf{Y}_R | \mathbf{Y}_D) = I(\mathbf{X}; \mathbf{Y}_R, \mathbf{Y}_D) - I(\mathbf{X}; \mathbf{Y}_D), \quad (55)$$

$$I(\mathbf{X}; \mathbf{Y}_R | \mathbf{Y}_D) = h(\mathbf{Y}_R|\mathbf{Y}_D) - h(\mathbf{Y}_R|\mathbf{Y}_D, \mathbf{X}). \quad (56)$$

The DoF of the first equality is  $DoF_R - DoF_D$ , while the DoF of the second is  $r' - r''$ . ■

We now further explore this connection via the concept of determinism in the relay channel. As already mentioned, for a relay channel with  $\mathbf{Y}_R = f(\mathbf{Y}_D, \mathbf{X})$ , compress-and-forward improves the rate in a 1:1 ratio of  $C_0$  as long as  $I(\mathbf{X}; \mathbf{Y}_R, \mathbf{Y}_D) > I(\mathbf{X}; \mathbf{Y}_D)$  for some  $p(\mathbf{x})$  [15]. A relay channel with  $\mathbf{Y}_R = f(\mathbf{Y}_D)$ , however, is reversely degraded

and its capacity, given by  $\max_{p(\mathbf{x})} I(\mathbf{X}; \mathbf{Y}_D)$ , does not depend on  $C_0$  [1].

For the MIMO relay channel considered here, when  $d \geq t + s$ , the channel (46)-(47) is reversely degraded, because

$$\tilde{\mathbf{Y}}_R = [H_{SR}H_{TR}] \left( \begin{bmatrix} H_{SD}^\dagger \\ H_{TD}^\dagger \end{bmatrix} [H_{SD}H_{TD}] \right)^{-1} \begin{bmatrix} H_{SD}^\dagger \\ H_{TD}^\dagger \end{bmatrix} \tilde{\mathbf{Y}}_D. \quad (57)$$

In this case, the slope of  $\bar{R}_{CF}(C_0)$  does not approach one.

When  $d < t + s$ , the channel (46)-(47) can contain deterministic components that are not reversely degraded. It turns out that the DoF-optimal distributed zero-forcing scheme mentioned in Section V can reveal such deterministic components. More specifically, we first form  $\tilde{\mathbf{Y}}'_R$ , defined to be the component of  $\tilde{\mathbf{Y}}_R$  that is independent of  $\tilde{\mathbf{Y}}_D$ , i.e.,

$$\begin{aligned} \tilde{\mathbf{Y}}'_R &= \tilde{\mathbf{Y}}_R - S_{\tilde{\mathbf{Y}}_R, \tilde{\mathbf{Y}}_D}^{(1,2)} S_{\tilde{\mathbf{Y}}_D}^{-1} \tilde{\mathbf{Y}}_D \\ &= [H_{SR}H_{TR}] \bar{P} \begin{bmatrix} \mathbf{X} \\ \mathbf{X}_t \end{bmatrix} \triangleq [\bar{H}_{SR}\bar{H}_{TR}] \begin{bmatrix} \mathbf{X} \\ \mathbf{X}_T \end{bmatrix}, \end{aligned} \quad (58)$$

where

$$\bar{P} = \mathbf{I}_{s+t} - \begin{bmatrix} S_{\mathbf{X}}H_{SD}^\dagger \\ S_{\mathbf{X}_T}H_{TD}^\dagger \end{bmatrix} S_{\tilde{\mathbf{Y}}_D}^{-1} [H_{SD}H_{TD}]. \quad (59)$$

is a projection matrix. Now, consider the effective channel

$$\begin{bmatrix} \tilde{\mathbf{Y}}'_R \\ \tilde{\mathbf{Y}}_D \end{bmatrix} = \begin{bmatrix} \bar{H}_{SR}\bar{H}_{TR} \\ H_{SD}H_{TD} \end{bmatrix} \begin{bmatrix} \mathbf{X} \\ \mathbf{X}_T \end{bmatrix}. \quad (60)$$

If  $r + d > t$ , then we can select a combining matrix  $\bar{C}_R \in \mathbb{C}^{(r+d-t)^+ \times r}$  such that

$$[\bar{C}_R \bar{A}] \begin{bmatrix} \bar{H}_{TR} \\ H_{TD} \end{bmatrix} = \mathbf{0}, \quad (61)$$

in which case

$$\bar{C}_R \tilde{\mathbf{Y}}'_R = [\bar{C}_R \bar{A}] \begin{bmatrix} \bar{H}_{SR} \\ H_{SD} \end{bmatrix} \mathbf{X} - \bar{A} \tilde{\mathbf{Y}}_D \quad (62)$$

is the component of  $\tilde{\mathbf{Y}}_R$  that is a function of  $(\tilde{\mathbf{Y}}_D, \mathbf{X})$ , but not a function of  $\tilde{\mathbf{Y}}_D$  alone. Such deterministic component gives rise to the unit slope of  $\bar{R}_{CF}(C_0)$  at  $C_0 = 0$ . It exists if and only if both  $r + d > t$  and  $d < s + t$ .

We now see that using distributed zero-forcing combining at the relay not only gives rise to DoF-optimal relaying strategy, but also reveals the deterministic components of the MIMO relay channel. It is for this reason that the condition for having DoF improvement by  $C_0 = \infty$  is the same as the condition under which relay has deterministic components and has  $\lim_{\sigma^2 \rightarrow 0} \frac{dR_{CF}(C_0)}{dC_0} = 1$  at small  $C_0$ .

From the DoF point of view, one can interpret the above conditions on the numbers of antennas in the following way. To improve DoF by adding  $r$  more antennas to the destination, the destination must not already have sufficient antennas to be able to completely mitigate interference and to resolve the intended signal, hence  $d < s + t$  is required. Further, the relay and the destination together must have enough antennas to mitigate all of the interference, so  $r + d > t$  is needed. Thus, we need  $r + d > t$  and  $d < s + t$ , as otherwise adding  $r$  more antennas to the receiver cannot improve the spatial DoF.

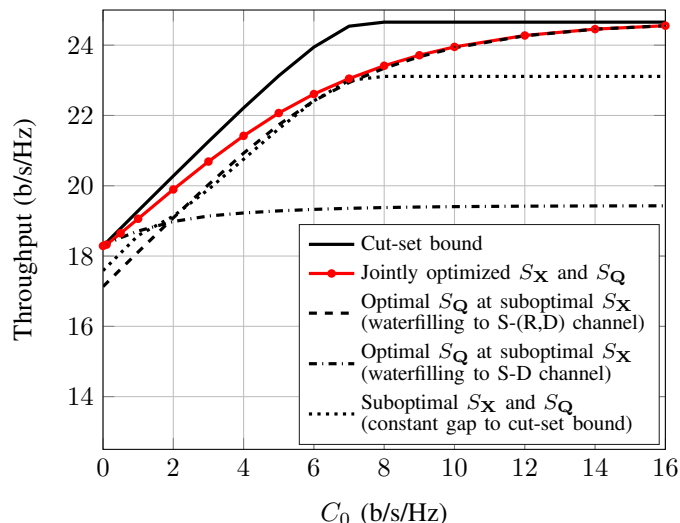


Fig. 4. Spectral efficiency versus relaying capacity  $C_0$  for the case where the source has three antennas ( $s = 3$ ), and the relay and destination are each equipped with two antennas ( $r = 2$  and  $d = 2$ ) with no inter-cell interference ( $t = 0$ ).

## VII. CONSTANT GAP CHARACTERIZATION OF CAPACITY

Throughout this paper, we have focused on the compress-and-forward relaying strategy with Gaussian input and quantization. In this final section of the paper, we show that this relaying strategy achieves the capacity of the Gaussian MIMO relay channel with noise correlation to within an additive gap that only depends on the number of antennas.

*Theorem 7:* For the MIMO relay channel under study, the achievable rate using optimized input and quantization covariance matrices given by Algorithm 1 is to within  $\min(r, s)$  bits of the capacity.

*Proof:* See Appendix E. ■

## VIII. NUMERICAL EXAMPLES

In this section, we provide numerical examples of MIMO relaying in a wireless cellular environment. We simulate a picocell network with a BS transmitting at a maximum power of 1W over 10MHz to a user located 100m away. A relay node, located 10m away from the user, pools antennas with user's receiver over a digital link of capacity  $C_0$ . Here,  $C_0$  is normalized by the 10MHz of bandwidth and is expressed in b/s/Hz. Interfering BSs are placed on a hexagonal grid, with minimum BS-to-BS distance of 200m. This scenario is shown in Fig. 1. The background noise power spectral density is  $-174$ dBm/Hz. Channel gains are simulated using  $L = 140.7 + 36.7 \log_{10}(d_{\text{km}})$  dB as the path loss model, log-normal shadowing with 10dB standard deviation, and Rayleigh fading [23].

### A. Relaying for Interference Mitigation and Signal Enhancement

Fig. 4 illustrates the effect of antenna pooling for enhancing the intended signal when there is no interference, so the noises at relay and destination are independent. It

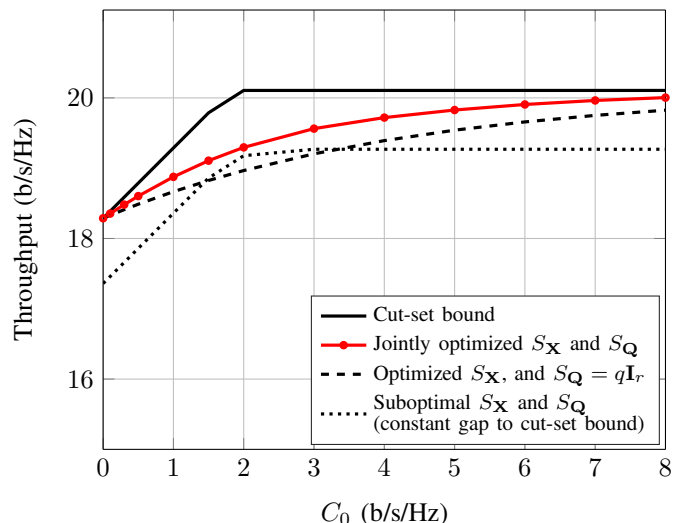


Fig. 5. Spectral efficiency versus relaying capacity  $C_0$  for the case where the source has two antennas ( $s = 2$ ), and the relay and destination are each equipped with three antennas ( $r = 3$  and  $d = 3$ ) with no inter-cell interference ( $t = 0$ ).

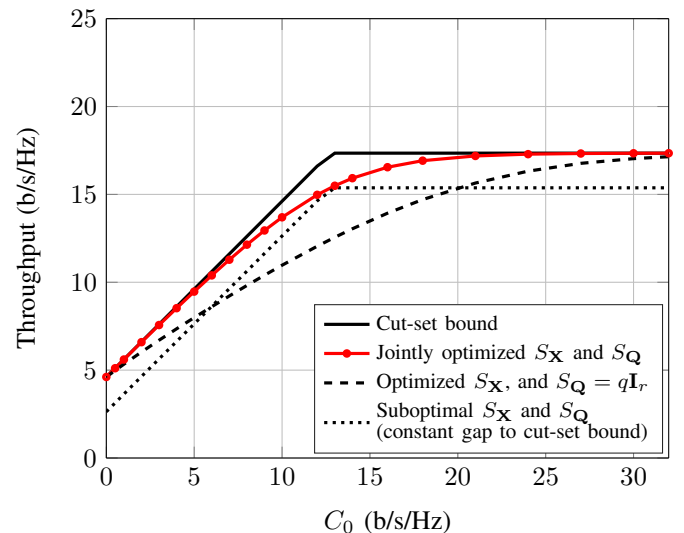


Fig. 6. Spectral efficiency versus relaying capacity  $C_0$  for the case where the source has two antennas ( $s = 2$ ), and the relay and destination are each equipped with three antennas ( $r = 3$  and  $d = 3$ ) with four inter-cell interference sources ( $t = 4$ ).

shows the rate improvement by relaying in a channel with  $(s, d, r, t) = (3, 2, 2, 0)$ . Without the relay, DoF is limited by the number of antennas at the destination, which is  $DoF_D = 2$ . Adding  $r = 2$  extra antennas to the destination improves DoF by  $\Delta DoF = 1$ . Also, this channel has 1 asymptotically deterministic component, and as shown in Fig. 4, at  $C_0 = 1$  b/s/Hz, the improvement in throughput by the optimized compress-and-forward is around 0.74 b/s/Hz. Here, antenna pooling improves the overall throughput considerably.

Fig. 4 also demonstrates the importance of optimizing the input covariance matrix. We plot the achievable rates for two suboptimal choices of input covariance: water-filling covariance of the source-to-destination and source-to-relay-

and-destination point-to-point channels. For these fixed input covariance matrices, we optimize the quantization noise covariance. Depending on the value of  $C_0$ , each of them can be strictly suboptimal. For small values of  $C_0$ , steering the beam toward destination is close to optimal. However, as  $C_0$  increases, this  $S_{\mathbf{X}}$  fails to achieve benefits of antenna pooling. For large values of  $C_0$ , steering the beam toward both relay and destination is close to optimal, but a gap exits at small  $C_0$ . Moreover, in this scenario, joint optimization of input and quantization noise outperforms the suboptimal evaluation of achievable rate for constant-gap capacity characterization by up to 6.5%.

Fig. 5 presents the results for a channel with  $(s, d, r, t) = (2, 3, 3, 0)$ . Without the relay, DoF is constrained by the number of BS antennas, not the number of antennas at the destination. Therefore, relaying does not increase the overall DoF. Also, as predicted by Theorem 6, the improvement in the overall rate is not notable. In this case, with  $C_0 = 7$  b/s/Hz, the throughput improvement is only around 1.7 b/s/Hz.

Fig. 6 considers the same setup as Fig. 5, except that now four interfering single-antenna BSs are added and we have  $(s, d, r, t) = (2, 3, 3, 4)$ . Due to interference, the rate at  $C_0 = 0$  is low, but the optimized use of the relaying link improves the throughput significantly. This is because, due to the common intercell interference, now the noises at the relay and at the destination are correlated. This noise correlation makes relaying effective for improving the rate. The maximum possible rate improvement is around 12.7 b/s/Hz, which is achieved at  $C_0 = 24$  b/s/Hz. Here, the DoF improvement with infinite  $C_0$  is  $\Delta DoF = 2$  and the channel has 2 asymptotically deterministic components. At around  $C_0 = 10$  b/s/Hz, the improvement in throughput is around 9.1 b/s/Hz. In this scenario, the improvement in rate by joint optimization of input and quantization noise covariance matrices over the suboptimal evaluation of rate for constant-gap capacity characterization is around 75% at small  $C_0$ 's and 12.8% at large  $C_0$ 's, illustrating the importance of optimizing quantization at low  $C_0$ 's. It is worth noting that the overall throughput at large  $C_0$  in Fig. 6 is close to the achievable rate of the  $C_0 = 0$  scenario in Figs. 4 and 5, illustrating the almost complete interference rejection capability of relaying.

Figs. 5 and 6 also demonstrate the importance of optimizing the quantization noise covariance matrix. The achievable rate for a simple suboptimal choice of  $S_{\mathbf{Q}} = q\mathbf{I}_r$  is included, where  $q$  is set to satisfy the relaying rate constraint with equality, for the optimized  $S_{\mathbf{X}}$  obtained from Algorithm 1. This simple choice of  $S_{\mathbf{Q}}$  results in a strictly suboptimal performance as shown in Figs. 5 and 6. In the scenario of Fig. 6, this simple choice of  $S_{\mathbf{Q}}$  results in a DoF loss as shown by Theorem 4.

### B. Effect of Numbers of Antennas on the Slope

We illustrate the effect of number of antennas at the relay ( $r$ ) and at the destination ( $d$ ) on the slope of compress-and-forward rate versus relaying link capacity  $\bar{R}_{CF}(C_0)$ . In this example, the source is equipped with five antenna and there are 18 interfering BSs each equipped with one antenna, i.e.,  $(s, t) = (5, 18)$ . Fig. 7 shows the value of  $1 - \frac{1}{\lambda_i}$  for

$i = 1, \dots, 6$ , which is the slope of  $\bar{R}_{CF}(C_0)$  at  $\bar{C}_i$  as in (35), averaged over 100 realizations of the channel and fixed transmit covariance  $S_{\mathbf{X}}$ .

Since the source has  $s = 5$  antennas, by Theorem 2, the 6<sup>th</sup> element of  $C_R \mathbf{Y}_R$  is always reversely degraded and its CSINR is zero, i.e.,  $\lambda_6 = 1$ . The optimal quantization does not quantize this element, because it cannot further improve the rate. In simulation results shown in Fig. 7(f), the slope of rate curve at  $\bar{C}_6$  is almost zero.

For  $i = 1, \dots, 5$ , by (43) in Theorem 3, when  $r$  and  $d$  are such that both  $r + d > 17 + i$  and  $d < 24 - i$ , the  $i^{\text{th}}$  element of  $C_R \mathbf{Y}_R$  is asymptotically deterministic. Hence, the value of  $1 - \frac{1}{\lambda_i}$  approaches 1 as the power of noise goes to zero. When  $d \geq 24 - i$  the  $i^{\text{th}}$  element of  $C_R \mathbf{Y}_R$  is asymptotically reversely degraded, and  $1 - \frac{1}{\lambda_i}$  does not approach 1. Also, when  $r + d \leq 17 + i$ , the 18-dimensional interference signal makes both  $S_{\mathbf{Y}_R|\mathbf{Y}_D, \mathbf{X}}$  and  $S_{\mathbf{Y}_R|\mathbf{Y}_D}$  full-rank, and keeps the slope  $1 - \frac{1}{\lambda_i}$  away from 1. These are indeed observed by numerical simulations in Figs. 7(a)-(e).

## IX. CONCLUSION

This paper considers MIMO relaying for interference mitigation and signal enhancement in a wireless communication network. Joint optimization of transmit and quantization noise covariance matrices in compress-and-forward scheme enables the receiver to efficiently utilize extra spatial dimensions from a relay node. This paper shows that this scheme achieves the capacity of the channel to within a constant gap that only depends on the numbers of antennas.

Optimizing the relay's quantization noise covariance matrix is crucial for efficient interference mitigation. This is the key step in characterizing the capacity of the MIMO relay channel to within a constant gap. It further reveals the asymptotically deterministic and reversely degraded components of the channel. When the channel has an asymptotically deterministic component, the slope of the optimized compress-and-forward rate  $\bar{R}_{CF}(C_0)$  at small  $C_0$  approaches its maximum of 1 at high SNR and INR. Optimizing relay's quantization enables achieving the maximum possible DoF of the channel through distributed zero-forcing of interference.

Antenna pooling is most efficient when the number of antennas at the source  $s$ , at the destination  $d$ , at the relay  $r$ , and the dimension of interference  $t$  satisfy both  $r + d > t$  and  $d < s + t$ ; otherwise, it does not improve the overall DoF at  $C_0 = \infty$ , and the slope of  $\bar{R}_{CF}(C_0)$  at small  $C_0$  does not approach the maximum of 1 at high SNR and INR. Typically, the number of antennas at a user device is small and the latter condition easily holds. The former condition points to the benefit of deploying a large number of antennas at the relay node, which enables distributed zero-forcing of the interference.

## APPENDIX A

The following lemma characterizes the scaling of eigenvalues of  $S_{\mathbf{Y}_R|\mathbf{Y}_D}$  and  $S_{\mathbf{Y}_R|\mathbf{Y}_D, \mathbf{X}}$  with the background noise power, as it goes to zero. It is used for counting the number of

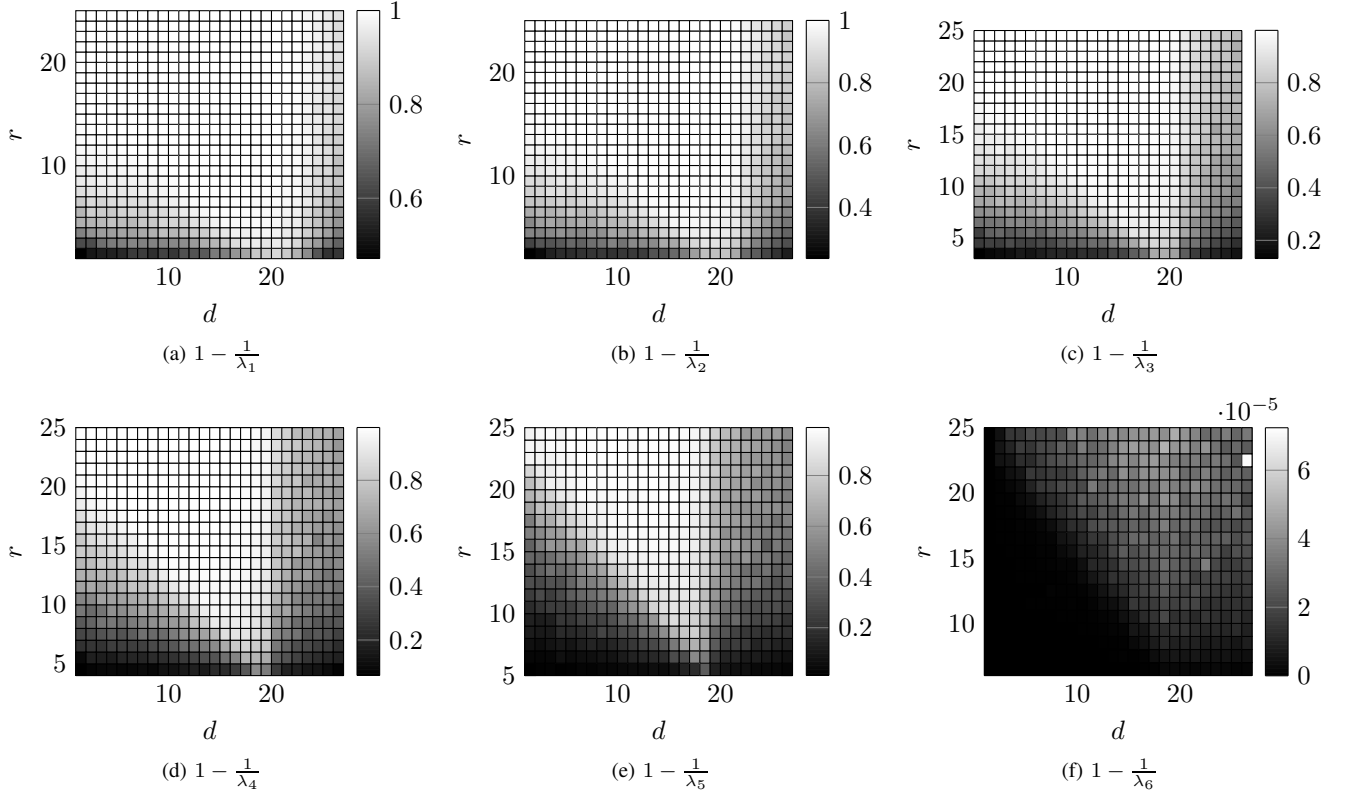


Fig. 7. Average slope of  $\bar{R}_{CF}(C_0)$  at  $\bar{C}_{0,i}$ , i.e.,  $1 - \frac{1}{\lambda_i}$ , for  $i = 1, \dots, 6$  as numbers of antennas at the destination ( $d$ ) and at the relay ( $r$ ) vary, with  $s = 5$  antennas at the source and  $t = 18$  single-antenna interference sources. Observe that the average slope at  $\bar{C}_{0,i}$  is close to 1 when  $r + d > t + i - 1$  and  $d < s + t - i + 1$  for  $i = 1, \dots, 5$ , and is close to zero for  $i = 6$ .

asymptotic deterministic components and for the DoF analysis in Appendices B to D.

*Lemma 3:* At the limit of high SNR and INR, i.e., as  $\sigma^2 \rightarrow 0$ , we have

$$\lambda_i(S_{\mathbf{Y}_R|\mathbf{Y}_D}) = \lambda_i(S_{\bar{\mathbf{Y}}_R|\bar{\mathbf{Y}}_D}) + a_i\sigma^2 + O(\sigma^4), \quad (63)$$

$$\lambda_i(S_{\mathbf{Y}_R|\mathbf{Y}_D,\mathbf{X}}) = \lambda_i(S_{\bar{\mathbf{Y}}_R|\bar{\mathbf{Y}}_D,\mathbf{X}}) + a'_i\sigma^2 + O(\sigma^4), \quad (64)$$

for positive  $a_i$ 's and  $a'_i$ 's. Here,  $\bar{\mathbf{Y}}_R$  and  $\bar{\mathbf{Y}}_D$  are as defined in (46)-(47).

*Proof:* Define  $L \triangleq \begin{bmatrix} H_{SD}S_{\mathbf{X}}^{\frac{1}{2}} & H_{TD}S_{\mathbf{X}_T}^{\frac{1}{2}} \end{bmatrix}$  and  $M \triangleq \begin{bmatrix} H_{SR}S_{\mathbf{X}}^{\frac{1}{2}} & H_{TR}S_{\mathbf{X}_T}^{\frac{1}{2}} \end{bmatrix}$ . We have

$$\begin{aligned} S_{\mathbf{Y}_R|\mathbf{Y}_D} & \stackrel{(a)}{=} S_{\bar{\mathbf{Y}}_R} + \sigma^2\mathbf{I}_r - ML^\dagger (LL^\dagger + \sigma^2\mathbf{I}_d)^{-1} LM^\dagger \\ & \stackrel{(b)}{=} S_{\bar{\mathbf{Y}}_R} + \sigma^2\mathbf{I}_r - MVD^\dagger (DD^\dagger + \sigma^2\mathbf{I}_d)^{-1} DV^\dagger M^\dagger \\ & \stackrel{(c)}{=} S_{\bar{\mathbf{Y}}_R} + \sigma^2\mathbf{I}_r - MVD^\dagger \\ & \quad \left( \sum_{n=0}^{\infty} (-\sigma^2)^n (DD^\dagger)^{-(n+1)} \right) DV^\dagger M^\dagger \\ & = S_{\bar{\mathbf{Y}}_R|\bar{\mathbf{Y}}_D} + \sigma^2\mathbf{I}_r - ML^\dagger \left( \sum_{n=1}^{\infty} (-\sigma^2)^n S_{\bar{\mathbf{Y}}_D}^{-(n+1)} \right) LM^\dagger \quad \text{and} \\ & \triangleq S_{\bar{\mathbf{Y}}_R|\bar{\mathbf{Y}}_D} + \sum_{n=1}^{\infty} (-1)^{n+1} \sigma^{2n} S_n, \end{aligned} \quad (65)$$

where, (a) follows by the Schur complement formula, (b) follows by the singular value decomposition (SVD)  $L = UDV^\dagger$ , and (c) follows by the Taylor expansion of each diagonal element.

Similar to the above, by taking SVD of  $H_{TD}S_{\mathbf{X}_T}^{\frac{1}{2}}$  one can write

$$S_{\mathbf{Y}_R|\mathbf{Y}_D,\mathbf{X}} = S_{\bar{\mathbf{Y}}_R|\bar{\mathbf{Y}}_D,\mathbf{X}} + \sum_{n=1}^{\infty} (-1)^{n+1} \sigma^{2n} S'_n. \quad (66)$$

All  $S_n$ 's and  $S'_n$ 's are positive semidefinite, and both  $S_1$  and  $S'_1$  are full-rank.

Since  $S_{\mathbf{Y}_R|\mathbf{Y}_D}$  and  $S_{\mathbf{Y}_R|\mathbf{Y}_D,\mathbf{X}}$  have convergent series in  $\sigma^2$  with Hermitian  $S_n$ 's and  $S'_n$ 's, the eigenvalues  $\lambda_i(S_{\mathbf{Y}_R|\mathbf{Y}_D})$  and  $\lambda_i(S_{\mathbf{Y}_R|\mathbf{Y}_D,\mathbf{X}})$  have convergent series in  $\sigma^2$  as well [24, Chapter 1]

$$\lambda_i(S_{\mathbf{Y}_R|\mathbf{Y}_D}) = \sum_{n=0}^{\infty} a_{i,n} \sigma^{2n}, \quad (67)$$

$$\lambda_i(S_{\mathbf{Y}_R|\mathbf{Y}_D,\mathbf{X}}) = \sum_{n=0}^{\infty} a'_{i,n} \sigma^{2n}. \quad (68)$$

Using Weyl's inequality [6, Theorem 4.3.1] over the summations in (65) and (66) inductively, we have

$$\begin{aligned} \lambda_i(S_{\bar{\mathbf{Y}}_R|\bar{\mathbf{Y}}_D}) + \sum_{n=1}^{\infty} (-1)^{n+1} \sigma^{2n} \lambda_r(S_n) &\leq \lambda_i(S_{\mathbf{Y}_R|\mathbf{Y}_D}) \\ &\leq \lambda_i(S_{\bar{\mathbf{Y}}_R|\bar{\mathbf{Y}}_D}) + \sum_{n=1}^{\infty} (-1)^{n+1} \sigma^{2n} \lambda_1(S_n), \end{aligned} \quad (69)$$

and

$$\begin{aligned} \lambda_i(S_{\bar{\mathbf{Y}}_R|\bar{\mathbf{Y}}_D,\mathbf{X}}) + \sum_{n=1}^{\infty} (-1)^{n+1} \sigma^{2n} \lambda_r(S'_n) &\leq \lambda_i(S_{\mathbf{Y}_R|\mathbf{Y}_D,\mathbf{X}}) \\ &\leq \lambda_i(S_{\bar{\mathbf{Y}}_R|\bar{\mathbf{Y}}_D,\mathbf{X}}) + \sum_{n=1}^{\infty} (-1)^{n+1} \sigma^{2n} \lambda_1(S'_n), \end{aligned} \quad (70)$$

By the squeeze theorem,  $a_{i,0} = \lambda_i(S_{\bar{\mathbf{Y}}_R|\bar{\mathbf{Y}}_D})$  and  $a'_{i,0} = \lambda_i(S_{\bar{\mathbf{Y}}_R|\bar{\mathbf{Y}}_D,\mathbf{X}})$ . Moreover,  $a_{i,1}$  and  $a'_{i,1}$  are positive, because both  $S_1$  and  $S'_1$  are positive definite matrices. ■

## APPENDIX B PROOF OF THEOREM 3

Before counting the number of asymptotic deterministic components, we characterize the rank of the two conditional covariance matrices in the following lemma.

*Lemma 4:* Consider  $\bar{\mathbf{Y}}_R$  and  $\bar{\mathbf{Y}}_D$  as defined in (46)-(47). We have  $\text{rank}(S_{\bar{\mathbf{Y}}_R|\bar{\mathbf{Y}}_D}) = \min(r, (s^r + t - d)^+)$  and  $\text{rank}(S_{\bar{\mathbf{Y}}_R|\bar{\mathbf{Y}}_D,\mathbf{X}}) = \min(r, (t - d)^+)$ , almost surely.

*Proof:* Since  $\text{rank}(S_{\mathbf{X}}) = s^r$  and  $\text{rank}(S_{\mathbf{X}_T}) = t$ , we have

$$\text{rank}(S_{\bar{\mathbf{Y}}_R,\bar{\mathbf{Y}}_D}) = \min(r + d, s^r + t), \quad (71)$$

$$\text{rank}(S_{\bar{\mathbf{Y}}_D}) = \min(d, s^r + t), \quad (72)$$

$$\text{rank}(S_{\bar{\mathbf{Y}}_R,\bar{\mathbf{Y}}_D,\mathbf{X}}) = s^r + \min(r + d, t), \quad (73)$$

$$\text{rank}(S_{\bar{\mathbf{Y}}_D,\mathbf{X}}) = s^r + \min(d, t). \quad (74)$$

By rank additivity of generalized Schur complement [25, Theorem 1]

$$\text{rank}(S_{\bar{\mathbf{Y}}_R|\bar{\mathbf{Y}}_D}) \leq \text{rank}(S_{\bar{\mathbf{Y}}_R,\bar{\mathbf{Y}}_D}) - \text{rank}(S_{\bar{\mathbf{Y}}_D}), \quad (75)$$

with equality if the null space of  $S_{\bar{\mathbf{Y}}_D}$  is a subset of the null space of  $S_{\bar{\mathbf{Y}}_R,\bar{\mathbf{Y}}_D}^{(1,2)}$ . When  $d \leq s^r + t$ ,  $S_{\bar{\mathbf{Y}}_D}$  is full-rank and has a trivial null space. When  $d \geq s^r + t$ , the right-hand-side of (75) is zero. Therefore, equality always holds in (75), and

$$\text{rank}(S_{\bar{\mathbf{Y}}_R|\bar{\mathbf{Y}}_D}) = \min(r, (s + t - d)^+). \quad (76)$$

Similarly, we have

$$\text{rank}(S_{\bar{\mathbf{Y}}_R|\bar{\mathbf{Y}}_D,\mathbf{X}}) \leq \text{rank}(S_{\bar{\mathbf{Y}}_R,\bar{\mathbf{Y}}_D,\mathbf{X}}) - \text{rank}(S_{\bar{\mathbf{Y}}_D,\mathbf{X}}), \quad (77)$$

with equality if the null space of  $S_{\bar{\mathbf{Y}}_D,\mathbf{X}}$  is a subset of the null space of  $S_{\bar{\mathbf{Y}}_R,\bar{\mathbf{Y}}_D,\mathbf{X}}^{(1,2)}$ . When  $d \leq t$ , the null space of

$$S_{\bar{\mathbf{Y}}_D,\mathbf{X}} = \begin{bmatrix} H_{SD}S_{\mathbf{X}}H_{SD}^\dagger + H_{TD}S_{\mathbf{X}_T}H_{TD}^\dagger & H_{SD}S_{\mathbf{X}} \\ S_{\mathbf{X}}H_{SD}^\dagger & S_{\mathbf{X}} \end{bmatrix}$$

is  $s - s^r$  dimensional and is caused by the rank deficiency of  $S_{\mathbf{X}}$ . Hence, it is a subset of the null space of

$$S_{\bar{\mathbf{Y}}_R,\bar{\mathbf{Y}}_D,\mathbf{X}}^{(1,2)} = [H_{SR}S_{\mathbf{X}}H_{SD}^\dagger + H_{TR}S_{\mathbf{X}_T}H_{TD}^\dagger \quad H_{SR}S_{\mathbf{X}}].$$

When  $d > t$ , the right-hand-side of (77) is zero. Therefore, we always have equality in (77), and

$$\text{rank}(S_{\bar{\mathbf{Y}}_R|\bar{\mathbf{Y}}_D,\mathbf{X}}) = \min(r, (t - d)^+). \quad (78)$$

Now, we proceed to prove Theorem 3.

*Proof:* The rank of the conditional covariance matrices  $S_{\bar{\mathbf{Y}}_R|\bar{\mathbf{Y}}_D}$  and  $S_{\bar{\mathbf{Y}}_R|\bar{\mathbf{Y}}_D,\mathbf{X}}$  in (33) and (34) are characterized in Lemma 4. Here, we argue that the largest  $i$  for which we have

$$\lim_{\sigma^2 \rightarrow 0} \lambda_i(S_{\mathbf{Y}_R|\mathbf{Y}_D} S_{\mathbf{Y}_R|\mathbf{Y}_D,\mathbf{X}}^{-1}) = \infty \quad (79)$$

is the difference of the two ranks,  $r' - r''$ . To relate the limit of the generalized eigenvalues to ranks of conditional covariances, we need to use bounds

$$\frac{\lambda_{r''+i}(S_{\mathbf{Y}_R|\mathbf{Y}_D})}{\lambda_{r''+1}(S_{\mathbf{Y}_R|\mathbf{Y}_D,\mathbf{X}})} \leq \lambda_i(S_{\mathbf{Y}_R|\mathbf{Y}_D} S_{\mathbf{Y}_R|\mathbf{Y}_D,\mathbf{X}}^{-1}), \quad (80)$$

$$\lambda_i(S_{\mathbf{Y}_R|\mathbf{Y}_D} S_{\mathbf{Y}_R|\mathbf{Y}_D,\mathbf{X}}^{-1}) \leq \frac{\lambda_1(S_{\mathbf{Y}_R|\mathbf{Y}_D})}{\lambda_{r-(i-1)}(S_{\mathbf{Y}_R|\mathbf{Y}_D,\mathbf{X}})}, \quad (81)$$

and

$$\lambda_i(S_{\mathbf{Y}_R|\mathbf{Y}_D} S_{\mathbf{Y}_R|\mathbf{Y}_D,\mathbf{X}}^{-1}) \leq \frac{\lambda_i(S_{\mathbf{Y}_R|\mathbf{Y}_D})}{\lambda_r(S_{\mathbf{Y}_R|\mathbf{Y}_D,\mathbf{X}})}, \quad (82)$$

due to [26, Corollary 2.5].

For  $i \leq r' - r''$ , we have  $\lambda_{r''+1}(S_{\bar{\mathbf{Y}}_R|\bar{\mathbf{Y}}_D,\mathbf{X}}) = 0$  and  $\lambda_{r''+i}(S_{\bar{\mathbf{Y}}_R|\bar{\mathbf{Y}}_D}) > 0$ . In this case, the  $i^{\text{th}}$  element is asymptotically deterministic, but not asymptotically reversely degraded. By taking limit from both sides of (80) and using Lemma 3, we have

$$\begin{aligned} \lim_{\sigma^2 \rightarrow 0} \lambda_i(S_{\mathbf{Y}_R|\mathbf{Y}_D} S_{\mathbf{Y}_R|\mathbf{Y}_D,\mathbf{X}}^{-1}) &\geq \lim_{\sigma^2 \rightarrow 0} \frac{\lambda_{r''+i}(S_{\mathbf{Y}_R|\mathbf{Y}_D})}{\lambda_{r''+1}(S_{\mathbf{Y}_R|\mathbf{Y}_D,\mathbf{X}})} \\ &= \lim_{\sigma^2 \rightarrow 0} \frac{\lambda_{r''+i}(S_{\bar{\mathbf{Y}}_R|\bar{\mathbf{Y}}_D) + a_{r''+i}\sigma^2}{a'_{r''+1}\sigma^2} = \infty. \end{aligned} \quad (83)$$

For  $i > r' - r'' = \min(r, s^r, (r + d - t)^+, (s^r + t - d)^+)$ , the generalized eigenvalues remain finite. To see this, we should consider three possible cases.

1) When  $i > s^r$ , by Theorem 2, the  $i^{\text{th}}$  element is reversely degraded and we have  $\lambda_i = 1$  at all values of  $\sigma^2$ .

2) When  $i > r + d - t$ , using (44)-(45) it is easy to see that  $r'' > r - i$  and  $r' > 0$ . Therefore, both  $\lambda_{r-i+1}(S_{\bar{\mathbf{Y}}_R|\bar{\mathbf{Y}}_D,\mathbf{X}}) > 0$  and  $\lambda_1(S_{\bar{\mathbf{Y}}_R|\bar{\mathbf{Y}}_D}) > 0$ . By Lemma 3 and (81)

$$\lim_{\sigma^2 \rightarrow 0} \lambda_i \leq \lim_{\sigma^2 \rightarrow 0} \frac{\lambda_1(S_{\bar{\mathbf{Y}}_R|\bar{\mathbf{Y}}_D,\mathbf{X}}) + a_1\sigma^2}{\lambda_{r-(i-1)}(S_{\bar{\mathbf{Y}}_R|\bar{\mathbf{Y}}_D,\mathbf{X}}) + a'_{r-(i-1)}\sigma^2} < \infty. \quad (84)$$

3) When  $i > s^r + t - d$ , using (44) it is easy to see that  $r' < i$ , therefore,  $\lambda_i(S_{\bar{\mathbf{Y}}_R|\bar{\mathbf{Y}}_D}) = 0$ . In this case, the  $i^{\text{th}}$  element is asymptotically reversely degraded. By Lemma 3 and (82)

$$\lim_{\sigma^2 \rightarrow 0} \lambda_i \leq \lim_{\sigma^2 \rightarrow 0} \frac{a_i\sigma^2}{\lambda_r(S_{\bar{\mathbf{Y}}_R|\bar{\mathbf{Y}}_D,\mathbf{X}}) + a'_r\sigma^2} < \infty. \quad (85)$$

■

APPENDIX C  
PROOF OF THEOREM 4

*Proof:* Fix the transmit covariance  $S_{\mathbf{X}}$  to a full-rank matrix. Consider i.i.d. quantization of elements of the relay's observed vector, i.e., set  $S_{\mathbf{Q}} = q\mathbf{I}_r$ . To calculate DoF gain due to compress-and-forward relaying (16), we select  $q$  such that the relaying capacity constraint in (9) is satisfied with equality

$$f_c(S_{\mathbf{X}}, q\mathbf{I}_r) = C_0(\rho). \quad (86)$$

Hence,  $q$  depends on  $\rho$ . To characterize the asymptotic scaling of such a  $q$  with  $\rho$  (or equivalently with  $\sigma^2$ ), we let

$$x = \lim_{\sigma^2 \rightarrow 0} \frac{\log(q)}{\log(\sigma^2)}, \quad (87)$$

and obtain

$$x = \begin{cases} \frac{\alpha}{r'}, & \alpha \leq r' \\ \frac{r+\alpha-r'}{r}, & \alpha \geq r' \end{cases}. \quad (88)$$

To see this, note that the pre-log factor of  $C_0(\rho)$  is  $\alpha$  in (15). For the pre-log factor of  $f_c(S_{\mathbf{X}}, q\mathbf{I}_r)$ , using Lemma 3 in Appendix A, as  $\sigma^2 \rightarrow 0$  we have

$$\begin{aligned} f_c(S_{\mathbf{X}}, q\mathbf{I}_r) &= \log \frac{|S_{\mathbf{Y}_R|\mathbf{Y}_D} + q\mathbf{I}_r|}{|q\mathbf{I}_r|} \\ &= \sum_{i=1}^{r'} \log \frac{\lambda'_i + a'_i \sigma^2 + O(\sigma^4) + \sigma^{2x}}{\sigma^{2x}} \\ &\quad + \sum_{i=r'+1}^r \log \frac{a'_i \sigma^2 + O(\sigma^4) + \sigma^{2x}}{\sigma^{2x}}. \end{aligned} \quad (89)$$

Therefore, the pre-log factor of  $f_c(S_{\mathbf{X}}, q\mathbf{I}_r)$  is

$$\lim_{\sigma^2 \rightarrow 0} \frac{f_c(S_{\mathbf{X}}, q\mathbf{I}_r)}{-\log(\sigma^2)} = r'x + (r-r')(x-1)^+. \quad (90)$$

Solving  $r'x + (r-r')(x-1)^+ = \alpha$ , yields  $x$ .

Now, the desired DoF gain is

$$\Delta DoF_{i.i.d.} = \lim_{\sigma^2 \rightarrow 0} \frac{I(\mathbf{X}; \hat{\mathbf{Y}}_R | \mathbf{Y}_D)}{-\log(\sigma^2)}. \quad (91)$$

Using Lemma 3, as  $\sigma^2 \rightarrow 0$ ,

$$\begin{aligned} I(\mathbf{X}; \hat{\mathbf{Y}}_R | \mathbf{Y}_D) &= \log \frac{|S_{\mathbf{Y}_R|\mathbf{Y}_D} + q\mathbf{I}_r|}{|S_{\mathbf{Y}_R|\mathbf{Y}_D, \mathbf{X}} + q\mathbf{I}_r|} \\ &= \sum_{i=1}^{r'} \log \frac{\lambda'_i + a'_i \sigma^2 + O(\sigma^4) + \sigma^{2x}}{\lambda'_i + a'_i \sigma^2 + O(\sigma^4) + \sigma^{2x}} \\ &\quad + \sum_{i=r'+1}^r \log \frac{\lambda'_i + a'_i \sigma^2 + O(\sigma^4) + \sigma^{2x}}{a'_i \sigma^2 + O(\sigma^4) + \sigma^{2x}} \\ &\quad + \sum_{i=r'+1}^r \log \frac{a'_i \sigma^2 + O(\sigma^4) + \sigma^{2x}}{a'_i \sigma^2 + O(\sigma^4) + \sigma^{2x}} \\ &= \sum_{i=r'+1}^{r'} \log \frac{\lambda'_i + a'_i \sigma^2 + \sigma^{2x}}{a'_i \sigma^2 + \sigma^{2x}} + O(1). \end{aligned} \quad (92)$$

Hence, the pre-log factor of  $I(\mathbf{X}; \hat{\mathbf{Y}}_R | \mathbf{Y}_D)$  is

$$\Delta DoF_{i.i.d.} = (r' - r'') \min(1, x) = (r' - r'') \min\left(1, \frac{\alpha}{r'}\right). \quad (93)$$

Finally, by comparing (43) and (50) we have  $r' - r'' = DoF_R - DoF_D$ . ■

APPENDIX D  
PROOF OF THEOREM 5

*Proof:* Using the cut-set upper bound (5), we have

$$\Delta DoF \leq \min(DoF_R - DoF_D, \alpha). \quad (94)$$

To almost surely achieve this upper bound by compress-and-forward, we transform  $\mathbf{Y}_R$  using a matrix  $\tilde{C}_R \in \mathbb{C}^{\tilde{r} \times r}$ , then describe  $\tilde{C}_R \mathbf{Y}_R$  by

$$\hat{\mathbf{Y}}_R = \tilde{C}_R \mathbf{Y}_R + \mathbf{Q}, \quad (95)$$

with  $\mathbf{Q} \sim \mathcal{CN}(\mathbf{0}_{\tilde{r} \times 1}, q\mathbf{I}_{\tilde{r}})$  independent of other variables and

$$\tilde{r} = \min(r, s, (r+d-t)^+). \quad (96)$$

Similar to the proof of Theorem 4 in Appendix C, we achieve

$$\begin{aligned} \Delta DoF &= \left( \text{rank}(\tilde{C}_R S_{\mathbf{Y}_R|\mathbf{Y}_D} \tilde{C}_R^\dagger) - \text{rank}(\tilde{C}_R S_{\mathbf{Y}_R|\mathbf{Y}_D, \mathbf{X}} \tilde{C}_R^\dagger) \right) \\ &\quad \cdot \min\left(1, \frac{\alpha}{\text{rank}(\tilde{C}_R S_{\mathbf{Y}_R|\mathbf{Y}_D} \tilde{C}_R^\dagger)}\right). \end{aligned} \quad (97)$$

In Theorem 4, without combining the relay's observed vector, we had  $\text{rank}(S_{\mathbf{Y}_R|\mathbf{Y}_D, \mathbf{X}}) = r''$  and  $\text{rank}(S_{\mathbf{Y}_R|\mathbf{Y}_D}) = r'$ . The key step here is to design the combining matrix  $\tilde{C}_R$  at the relay such that  $\text{rank}(\tilde{C}_R S_{\mathbf{Y}_R|\mathbf{Y}_D, \mathbf{X}} \tilde{C}_R^\dagger) = 0$ , while  $\text{rank}(\tilde{C}_R S_{\mathbf{Y}_R|\mathbf{Y}_D} \tilde{C}_R^\dagger) = r' - r''$ . This can be obtained by distributed zero-forcing of interference, i.e.,  $\tilde{C}_R$  is such that for some  $A \in \mathbb{C}^{\tilde{r} \times d}$ ,

$$\begin{bmatrix} \tilde{C}_R & A \end{bmatrix} \begin{bmatrix} H_{TR} \\ H_{TD} \end{bmatrix} S_{\mathbf{X}_T}^{\frac{1}{2}} = \mathbf{0}, \quad (98)$$

while

$$\text{rank}\left(\begin{bmatrix} \tilde{C}_R & A \end{bmatrix} \begin{bmatrix} H_{SR} \\ H_{SD} \end{bmatrix} S_{\mathbf{X}}^{\frac{1}{2}}\right) = \tilde{r}, \quad (99)$$

almost surely. In other words,  $\tilde{C}_R$  is chosen such that the observed interference at the relay is aligned with the row space of the observed interference at the destination, i.e.,

$$\text{rowspan}\left(\tilde{C}_R H_{TR} S_{\mathbf{X}_T}^{\frac{1}{2}}\right) \subseteq \text{rowspan}\left(H_{TD} S_{\mathbf{X}_T}^{\frac{1}{2}}\right). \quad (100)$$

Note that since  $[H_{TR}^\dagger \ H_{TD}^\dagger]^\dagger S_{\mathbf{X}_T}^{\frac{1}{2}}$  has an  $(r+d-t)^+$  dimensional left null space, such a zero-forcing matrix always exists. Now, we argue that  $\text{rank}(\tilde{C}_R S_{\mathbf{Y}_R|\mathbf{Y}_D, \mathbf{X}} \tilde{C}_R^\dagger) = 0$  and  $\text{rank}(\tilde{C}_R S_{\mathbf{Y}_R|\mathbf{Y}_D} \tilde{C}_R^\dagger) = r' - r''$ .

We have

$$\begin{aligned} S_{\tilde{C}_R \mathbf{Y}_R, \mathbf{Y}_D} &= \begin{bmatrix} \tilde{C}_R H_{SR} \\ H_{SD} \end{bmatrix} S_{\mathbf{X}} \begin{bmatrix} H_{SR}^\dagger \tilde{C}_R^\dagger & H_{SD}^\dagger \end{bmatrix} \\ &\quad + \begin{bmatrix} \tilde{C}_R H_{TR} \\ H_{TD} \end{bmatrix} S_{\mathbf{X}_T} \begin{bmatrix} H_{TR}^\dagger \tilde{C}_R^\dagger & H_{TD}^\dagger \end{bmatrix}, \end{aligned} \quad (101)$$

and

$$\text{rank}(S_{\tilde{C}_R \tilde{\mathbf{Y}}_R, \tilde{\mathbf{Y}}_D}) = \min(\tilde{r} + d, \min(s, \tilde{r} + d) + \min(d, t)), \quad (102)$$

almost surely. Similar to the proof of Lemma 4, by rank additivity of generalized Schur complement

$$\begin{aligned} \text{rank}\left(\tilde{C}_R S_{\tilde{\mathbf{Y}}_R | \tilde{\mathbf{Y}}_D} \tilde{C}_R^\dagger\right) &= \text{rank}\left(S_{\tilde{C}_R \tilde{\mathbf{Y}}_R, \tilde{\mathbf{Y}}_D}\right) - \text{rank}\left(S_{\tilde{\mathbf{Y}}_D}\right) \\ &= \min(\tilde{r} + d, d + s, s + t) - \min(d, s + t) = r' - r''. \end{aligned} \quad (103)$$

Also, we have

$$\text{rank}\left(S_{\tilde{C}_R \tilde{\mathbf{Y}}_R, \tilde{\mathbf{Y}}_D, \mathbf{X}}\right) = s' + \min(d, t) = \text{rank}\left(S_{\tilde{\mathbf{Y}}_D, \mathbf{X}}\right), \quad (104)$$

almost surely. Similar to the proof of Lemma 4, by rank additivity of generalized Schur complement

$$\begin{aligned} \text{rank}\left(\tilde{C}_R S_{\tilde{\mathbf{Y}}_R | \tilde{\mathbf{Y}}_D, \mathbf{X}} \tilde{C}_R^\dagger\right) \\ = \text{rank}\left(S_{\tilde{C}_R \tilde{\mathbf{Y}}_R, \tilde{\mathbf{Y}}_D, \mathbf{X}}\right) - \text{rank}\left(S_{\tilde{\mathbf{Y}}_D, \mathbf{X}}\right) = 0. \end{aligned} \quad (105)$$

Therefore, the DoF gain (97) can be written as

$$\begin{aligned} \Delta DoF &= (r' - r'') \min\left(1, \frac{\alpha}{r' - r''}\right) \\ &= \min(DoF_R - DoF_D, \alpha). \end{aligned} \quad (106)$$

The last equality follows by noting  $r' - r'' = DoF_R - DoF_D$  from (43) and (50). ■

#### APPENDIX E PROOF OF THEOREM 7

*Proof:* We first argue that a sub-optimal evaluation of compress-and-forward rate in (8) is to within a constant gap of the cut-set upper bound (5). Then, we show that this is true for the achievable rate expression (6) when optimized by Algorithm 1 as well.

Let  $\mathbf{X} \sim \mathcal{CN}(\mathbf{0}_{s \times 1}, S_{\mathbf{X}, \text{CSB}}^*)$ , where  $S_{\mathbf{X}, \text{CSB}}^*$  is the global maximizer of the cut-set bound (5). Then, consider matrix  $C_R$  that simultaneously diagonalizes  $S_{\mathbf{Y}_R | \mathbf{Y}_D, \mathbf{X}}$  and  $S_{\mathbf{Y}_R | \mathbf{Y}_D, \mathbf{X}}$ , and the generalized eigenvalues  $\lambda_i$ 's in decreasing order as introduced in Lemma 1. Let  $\mathbf{Q} \sim \mathcal{CN}(\mathbf{0}_{r \times 1}, S_{\mathbf{Q}, \text{CG}})$ , where  $S_{\mathbf{Q}, \text{CG}} \triangleq C_R^{-\dagger} \Sigma_{\mathbf{Q}, \text{CG}} C_R^{-1}$  with diagonal  $\Sigma_{\mathbf{Q}, \text{CG}}$  such that the  $i^{\text{th}}$  diagonal element is

$$\Sigma_{\mathbf{Q}, \text{CG}}^{ii} = \begin{cases} \frac{\lambda_i}{\lambda_i - 1} & \lambda_i > 1 \\ +\infty & \lambda_i = 1 \end{cases}. \quad (107)$$

Under the above input and quantization distributions, the gap between the cut-set upper bound (5) and the achievable rate (8) is bounded as below

$$\begin{aligned} &\min\{I(\mathbf{X}; \mathbf{Y}_R, \mathbf{Y}_D), I(\mathbf{X}; \mathbf{Y}_D) + C_0\} \\ &\quad - \min\left\{I(\mathbf{X}; \hat{\mathbf{Y}}_R, \mathbf{Y}_D), \right. \\ &\quad \quad \left. I(\mathbf{X}; \mathbf{Y}_D) + C_0 - I(\mathbf{Y}_R; \hat{\mathbf{Y}}_R | \mathbf{Y}_D, \mathbf{X})\right\} \\ &\leq \max\left\{I(\mathbf{X}; \mathbf{Y}_R | \mathbf{Y}_D) - I(\mathbf{X}; \hat{\mathbf{Y}}_R | \mathbf{Y}_D), \right. \\ &\quad \quad \left. I(\mathbf{Y}_R; \hat{\mathbf{Y}}_R | \mathbf{Y}_D, \mathbf{X})\right\} \\ &= \max\left\{\log \frac{|S_{\mathbf{Y}_R | \mathbf{Y}_D}| \cdot |S_{\mathbf{Q}} + S_{\mathbf{Y}_R | \mathbf{Y}_D, \mathbf{X}}|}{|S_{\mathbf{Y}_R | \mathbf{Y}_D, \mathbf{X}}| \cdot |S_{\mathbf{Q}} + S_{\mathbf{Y}_R | \mathbf{Y}_D}|}, \right. \\ &\quad \quad \left. \log \frac{|S_{\mathbf{Q}} + S_{\mathbf{Y}_R | \mathbf{Y}_D, \mathbf{X}}|}{|S_{\mathbf{Q}}|}\right\} \\ &\stackrel{(a)}{=} \max\left\{\sum_{i=1}^r \log \frac{\lambda_i (\Sigma_{\mathbf{Q}}^{ii} + 1)}{\Sigma_{\mathbf{Q}}^{ii} + \lambda_i}, \sum_{i=1}^r \log \frac{\Sigma_{\mathbf{Q}}^{ii} + 1}{\Sigma_{\mathbf{Q}}^{ii}}\right\} \\ &\leq \sum_{i=1}^r \max\left(\log \frac{\lambda_i (\Sigma_{\mathbf{Q}}^{ii} + 1)}{\Sigma_{\mathbf{Q}}^{ii} + \lambda_i}, \log \frac{\Sigma_{\mathbf{Q}}^{ii} + 1}{\Sigma_{\mathbf{Q}}^{ii}}\right) \\ &\stackrel{(b)}{=} \sum_{i=1}^r \log\left(2 - \frac{1}{\lambda_i}\right) \stackrel{(c)}{\leq} r - (r - s)^+ = \min(r, s). \end{aligned} \quad (108)$$

Here, Lemma 1 is used in equality (a), equality (b) follows by the choice of  $\Sigma_{\mathbf{Q}}$  in (107); note that for  $i \in \{1, \dots, r\}$ , if  $\lambda_i > 1$ , the first and the second arguments of the maximization are, respectively, increasing and decreasing in  $\Sigma_{\mathbf{Q}}^{ii}$ . Therefore, the corresponding term is minimized by equating the two and solving for  $\Sigma_{\mathbf{Q}}^{ii}$ . If  $\lambda_i = 1$ , the corresponding term is zero by letting  $\Sigma_{\mathbf{Q}}^{ii} \rightarrow \infty$ . By Theorem 2, the number of such components is at least  $(r - s)^+$ , hence (c).

Now, we argue that the achievable rate by Algorithm 1 is also to within a constant gap of the cut-set bound. Initialize Algorithm 1 with  $S_{\mathbf{X}, \text{CSB}}^*$  and update the optimal quantization noise covariance, denoted by  $S_{\mathbf{Q}}^*$ . By [18, Theorem 16.4],  $S_{\mathbf{Q}}^*$  is the global optimum of (8) at  $S_{\mathbf{X}} = S_{\mathbf{X}, \text{CSB}}^*$  as well. Hence, the achievable rate by Algorithm 1, i.e.,  $R_{CF} = I(\mathbf{X}; \hat{\mathbf{Y}}_R, \mathbf{Y}_D)$  evaluated at  $(S_{\mathbf{X}, \text{CSB}}^*, S_{\mathbf{Q}}^*)$ , is no smaller than (8) evaluated at  $(S_{\mathbf{X}, \text{CSB}}^*, S_{\mathbf{Q}, \text{CG}})$ , which is already shown to be within  $\min(r, s)$  bits of the cut-set upper bound. ■

#### ACKNOWLEDGMENT

We thank Professor Jun Chen for informing us of [8].

#### REFERENCES

- [1] T. Cover and A. El Gamal, "Capacity theorems for the relay channel," *IEEE Trans. Inf. Theory*, vol. 25, no. 5, pp. 572–584, Sep. 1979.
- [2] G. Kramer, M. Gastpar, and P. Gupta, "Cooperative strategies and capacity theorems for relay networks," *IEEE Trans. Inf. Theory*, vol. 51, no. 9, pp. 3037 – 3063, Sept. 2005.
- [3] L. Zhang, J. Jiang, A. Goldsmith, and S. Cui, "Study of Gaussian relay channels with correlated noises," *IEEE Trans. Commun.*, vol. 59, no. 3, pp. 863–876, Mar. 2011.

- [4] S. Simoens, O. Muoz-Medina, J. Vidal, and A. del Coso, "Compress-and-forward cooperative MIMO relaying with full channel state information," *IEEE Trans. Signal Process.*, vol. 58, no. 2, pp. 781–791, Feb. 2010.
- [5] M. Gastpar, P. Dragotti, and M. Vetterli, "The distributed Karhunen-Loève transform," *IEEE Trans. Inf. Theory*, vol. 52, no. 12, pp. 5177 – 5196, Dec. 2006.
- [6] R. A. Horn and C. R. Johnson, *Matrix Analysis*. Cambridge University Press, 1990.
- [7] S. A. Ayoughi and W. Yu, "Optimized MIMO transmission and compression for interference mitigation with user cooperation," in *Proc. IEEE Int. Conf. Commun. (ICC)*, 2015.
- [8] C. Tian and J. Chen, "Remote vector Gaussian source coding with decoder side information under mutual information and distortion constraints," *IEEE Trans. Inf. Theory*, vol. 55, no. 10, pp. 4676–4680, Oct. 2009.
- [9] L. Zhou and W. Yu, "Capacity of the Gaussian relay channel with correlated noises to within a constant gap," *IEEE Commun. Lett.*, vol. 16, no. 1, pp. 2–5, Nov. 2012.
- [10] X. Jin and Y. Kim, "The approximate capacity of the MIMO relay channel," *IEEE Trans. Inf. Theory*, vol. 63, no. 2, pp. 1167–1176, 2017.
- [11] S. Mohajer, S. N. Diggavi, C. Fragouli, and D. N. C. Tse, "Approximate capacity of a class of Gaussian interference-relay networks," *IEEE Trans. Inf. Theory*, vol. 57, no. 5, pp. 2837–2864, 2011.
- [12] T. Gou, S. A. Jafar, C. Wang, S.-W. Jeon, and S.-Y. Chung, "Aligned interference neutralization and the degrees of freedom of the  $2 \times 2 \times 2$  interference channel," *IEEE Trans. Inf. Theory*, vol. 58, no. 7, pp. 4381–4395, 2012.
- [13] B. Rankov and A. Wittneben, "Spectral efficient protocols for half-duplex fading relay channels," *IEEE J. Sel. Areas Commun.*, vol. 25, no. 2, pp. 379–389, 2007.
- [14] K. S. Gomadam and S. A. Jafar, "The effect of noise correlation in amplify-and-forward relay networks," *IEEE Trans. Inf. Theory*, vol. 55, no. 2, pp. 731–745, 2009.
- [15] T. M. Cover and Y. Kim, "Capacity of a class of deterministic relay channel," Jun. 2007, pp. 591–595.
- [16] S. A. Ayoughi and W. Yu, "A DoF analysis of compress-and-forward in MIMO Gaussian relay channel with correlated noises," in *Proc. Can. Workshop Inf. Theory (CWIT)*, 2015.
- [17] A. Sanderovich, S. Shamai, Y. Steinberg, and G. Kramer, "Communication via decentralized processing," *IEEE Trans. Inf. Theory*, vol. 54, no. 7, pp. 3008–3023, 2008.
- [18] A. El Gamal and Y. Kim, *Network Information Theory*. Cambridge University Press, 2011.
- [19] D. P. Bertsekas, *Nonlinear Programming*. Athena Scientific, 2003.
- [20] C. R. Rao, *Linear Statistical Inference and Its Applications*, 2nd ed. Wiley, 1973.
- [21] A. del Coso and S. Simoens, "Distributed compression for MIMO coordinated networks with a backhaul constraint," *IEEE Trans. Wireless Commun.*, vol. 8, no. 9, pp. 4698–4709, Sep. 2009.
- [22] S. Boyd and L. Vandenberghe, *Convex Optimization*. Cambridge University Press, 2004.
- [23] *Further advancements for E-UTRA physical layer aspects*, 3GPP TS 36.814, E-UTRA, 3 2010, v9.0.0.
- [24] F. Rellich, *Perturbation theory of eigenvalue problems*. CRC Press, 1969.
- [25] D. Carlson, E. Haynsworth, and T. Markham, "A generalization of the Schur complement by means of the Moore-Penrose inverse," *SIAM J. Appl. Math.*, vol. 26, no. 1, pp. 169–175, Jan. 1974.
- [26] L.-Z. Lu and C. E. M. Pearce, "Some new bounds for singular values and eigenvalues of matrix products," *Ann. Operations Res.*, vol. 98, no. 1-4, pp. 141–148, 2000.